



HAL
open science

Indian mustard bioproducts dry-purification with natural adsorbents - A biorefinery for a green circular economy

Graeme Rapp, Victor Garcia-Montoto, Brice Bouyssière, Sophie Thiebaud-Roux, Alejandro Montoya, Richard Trethowan, Peter Pratt, Kevin Mozet, Jean-François Portha, Lucie Coniglio

► To cite this version:

Graeme Rapp, Victor Garcia-Montoto, Brice Bouyssière, Sophie Thiebaud-Roux, Alejandro Montoya, et al.. Indian mustard bioproducts dry-purification with natural adsorbents - A biorefinery for a green circular economy. *Journal of Cleaner Production*, 2021, 286, pp.125411. 10.1016/j.jclepro.2020.125411 . hal-03097316

HAL Id: hal-03097316

<https://univ-pau.hal.science/hal-03097316>

Submitted on 2 Jan 2023

HAL is a multi-disciplinary open access archive for the deposit and dissemination of scientific research documents, whether they are published or not. The documents may come from teaching and research institutions in France or abroad, or from public or private research centers.

L'archive ouverte pluridisciplinaire **HAL**, est destinée au dépôt et à la diffusion de documents scientifiques de niveau recherche, publiés ou non, émanant des établissements d'enseignement et de recherche français ou étrangers, des laboratoires publics ou privés.



Distributed under a Creative Commons Attribution - NonCommercial 4.0 International License

Indian mustard bioproducts dry-purification with natural adsorbents - a biorefinery for a green circular economy

Graeme Rapp^a, *Victor Garcia-Montoto*^b, *Brice Bouyssiere*^b, *Sophie Thiebaud-Roux*^c, *Alejandro Montoya*^d, *Richard Trethowan*^a, *Peter Pratt*^e, *Kevin Mozet*^f, *Jean-François Portha*^f, *Lucie Coniglio*^{f*}

^a The University of Sydney, Plant Breeding Institute, I.A. Watson International Grains Research Centre, PO Box 219, Narrabri, NSW 2390, Australia; graeme.rapp@sydney.edu.au (Graeme Rapp); richard.trethowan@sydney.edu.au (Richard Trethowan)

^b CNRS / UNIV Pau & Pays de l'Adour, Institut des Sciences Analytiques et de Physico-Chimie pour l'Environnement et les Matériaux, UMR 5254, 64000 Pau, France; victor.garcia-montoto@etud.univ-pau.fr (Victor Garcia-Montoto); brice.bouyssiere@univ-pau.fr (Brice Bouyssiere)

^c Laboratoire de Chimie Agro-Industrielle, LCA, Université de Toulouse, INRA, INP, Toulouse, France; sophie.thiebaudroux@ensiacet.fr (Sophie Thiebaud-Roux)

^d School of Chemical and Biomolecular Engineering, The University of Sydney, NSW 2006, Australia; alejandro.montoya@sydney.edu.au (Alejandro Montoya)

^e Valtris Enterprises France, Z.I. Baleycourt CS 10095, 55103 Verdun Cedex, France; peter.pratt@valtris.com (Peter Pratt)

^f Université de Lorraine - Ecole Nationale Supérieure des Industries Chimiques de Nancy, Laboratoire Réactions et Génie des Procédés UMR CNRS 7274, 1, rue Grandville BP 20451, 54001 Nancy Cedex, France; kevin.mozet@univ-lorraine.fr (Kevin Mozet); jean-francois.portha@univ-lorraine.fr (Jean-François Portha); lucie.coniglio@univ-lorraine.fr (Lucie Coniglio).

* To whom correspondence should be addressed.

Abstract

Processes based on homogeneous catalysts are the most widely used for industrial production of fatty acid derivatives, despite catalyst loss in aqueous effluents during the wet-purification stage. In this work, dry-purification of the crude bioproducts; ethyl biodiesel and biolubricants, derived from Indian mustard was conducted using various natural mineral (clay) and organic (plant issue) adsorbents to evaluate operating conditions including temperature, contact time and number of treatment cycles and to define the optimal procedure. Adsorbent characterization was determined by average particle size assessed using laser granulometry, morphology and elemental chemical composition measured by scanning electron spectroscopy with microanalysis using energy dispersive X-ray spectroscopy, chemical structure determination based on Fourier Transform InfraRed spectroscopy and porosity and specific area assessed using carbon dioxide or nitrogen adsorption. The quality of the biofuel and biolubricants, before and after dry-purification on the above adsorbents, was evaluated using different methods including Karl Fischer titration, gas chromatography with a flame ionization detector and inductively coupled plasma-atomic emission spectroscopy. Montmorillonite clay and finely ground Indian mustard stems (particle size of 100 to 710 μm) without further pyrolysis or carbonization treatment were found to be the best adsorbents. Combined with the selected dry-purification procedure (35-45°C, 20 min, single treatment cycle), most impurities including residual glycerides, free glycerin, water, catalysts and metals were removed from the resultant ethyl biodiesel thus meeting the basic biofuel specifications of acid value, color, density, viscosity, flash point, pour point, cloud point, cold filter plugging point, higher heating value, and oxidation stability. Further purification of biolubricants was required using bubble-washing with citric acid and vacuum distillation to obtain a product with acceptable density, viscosity and color. This work highlights the potential of a biorefinery system focused on Indian mustard contributing to a green circular economy, that would benefit both farmers and consumers in the respect of environment; farmers would gain in energy security and flexibility by biofuel, biolubricant and other bioproducts on-farm production, while ensuring healthy food security and offering job opportunities, the whole with reduced chemical and energy inputs and minimized waste effluents.

Keywords: dry-purification; ethyl biodiesel; biolubricant; Indian mustard; biorefinery concept; low cost production; limited environmental footprint.

Abbreviations

2D-NLDFT	Two-dimensional non-local density functional theory
2EH	2-ethyl-1-hexanol
AES	Atomic Emission Spectrometry
AUD	Australian dollar
BET	Brunauer-Emmet-Teller
C16:0	Ethyl or 2-ethylhexyl palmitate
C18:0	Ethyl or 2-ethylhexyl stearate
C18:1	Ethyl or 2-ethylhexyl oleate or <i>cis</i> -vaccenate
C18:2	Ethyl or 2-ethylhexyl linoleate
C18:3	Ethyl or 2-ethylhexyl linolenate
C20:1	Ethyl or 2-ethylhexyl gadoleate
C22:1	Ethyl or 2-ethylhexyl erucate
cFIMS	Fine Indian mustard stems after carbonization
cMIMS	Medium Indian mustard stems after carbonization
D	Vacuum distillation
DGs	Diacylglycerides
DPI	Department of Primary Industries
EDS	Energy dispersive X-ray spectroscopy
FFAs	Free fatty acids
FID	Flame ionization detector
FIMS	Fine Indian mustard stems
GC	Gas-chromatography
GHG	Greenhouse gas
GLSs	Glucosinolates
IMSO	Indian mustard seed oil
IMSO2EHE	Indian mustard seed oil 2-ethylhexyl ester (biolubricant)
IMSOEEs	Indian mustard seed oil ethyl esters (ethyl biodiesel)
IUPAC	International Union of Pure and Applied Chemistry
MGs	Monoacylglycerides
MIMS	Medium Indian mustard stems
Mt	Montmorillonite
NSW	New South Wales
pFIMS	Fine Indian mustard stems after pyrolysis

pMIMS	Medium Indian mustard stems after pyrolysis
PSD	Particle size distribution
SEM	Scanning electron microscopy
TGs	Triacylglycerides
W	Bubble-washing

1. Introduction

Indian mustard (*Brassica juncea*) is a hardy, drought and insect resistant species that can be incorporated into winter cereal and legume crop sequences (Kirkegaard and Sarwar, 1999). Indeed, its biofumigation properties provide chemical-free disease suppression in subsequent crops and can even increase yields by acting as a natural fertilizer (Ngala et al., 2015). Hence, Indian mustard does not compete with food crops but rather contribute to their proper development. Moreover, selective breeding of Indian mustard has produced genotypes with very high oil yields that are rich in unsaturated fatty acids, even in adverse environmental conditions such as drought and high ambient temperatures (Rapp, 2018). Nonetheless, under cool and/or wet environmental conditions, erucic acid levels higher than the maximum content of 2% recommended in edible oils by the European Food Safety Authority may be encountered (Vetter et al., 2020). Cultivation of Indian mustard as a rotational crop for oil production also provides other valuable components that have potential uses in an integrated biorefinery. These include pharmaceutical, veterinary, agricultural and animal food products derived from mustard meal high in glucosinolate concentration, protein and fibre (Rapp, 2018). Besides, bioethanol and biogas can be obtained from digestion of Indian mustard residues (Chen et al., 2019). Hence, Indian mustard cultivation may help the sustainability of farm crop rotations while generating additional regional economic benefits. In addition, apart from its applications in the food, pharmaceutical and veterinary fields, Indian mustard has shown great potential for phytoremediation as an effective and sustainable alternative for soil decontamination (Raj et al., 2020). This work aims to determine if Indian mustard can be harnessed within a biorefinery system to generate energy carriers and high value-added products that are additional to its benefits, whether grown in rotation under various climatic conditions or used for soil remediation. Therefore, although applied to edible Indian mustard oil, the present work aims to be extended to Indian mustard yielding vegetable

oil with high contents in erucic acid and/or used for phytoremediation. Two options of harnessing Indian mustard oil were targeted; firstly, the production of ethyl biodiesel as the energy carrier and secondly, the conversion of ethyl biodiesel into high value-added biolubricants. **Chen et al. (2019)** proposed low cost and environmentally-friendly conversion processes using a common reaction route; potassium hydroxide-based transesterification. Such processes offer valuable flexibility as crude oil prices fluctuate and the global demand for biolubricants is expected to increase up to 14 million tons in 2020 (**Hossain et al., 2018**). As example, the annual consumption of metalworking fluids used as lubricants in machining processes is estimated to be over two billion gallons in North America and 320,000 tons Europe. Moreover, out of those numbers, at least two thirds need to be disposed (**Syahir et al., 2017**); hence the urgency to shift towards biolubricants.

Further to the Indian mustard oil conversion technics proposed by **Chen et al. (2019)**, this paper focusses on optimizing the purification stage of the resulting crude bioproducts (biofuel and biolubricant) by using various natural mineral (clay) and organic (plant issue) adsorbents. The dry treatment procedure and the efficiency of the adsorbents in the removal of specific impurities such as glycerides, free glycerin, water, catalyst and metals without introducing contaminants was evaluated by characterization of the biofuel and biolubricant samples obtained before and after treatment. Structure and composition of adsorbents were analyzed to determine the relationship between structure and adsorption efficiency. The whole of information thus collected from characterization of the liquid bioproducts and adsorbents is expected to identify adsorbents suitable for the dry-purification procedure and to determine if a wet-purification stage, such as bubble-washing and vacuum distillation, was required to obtain liquid bioproducts with adequate functional properties.

The novelty of this paper aimed at optimizing the purification stage of ethyl biodiesel and biolubricants production processes from Indian mustard is on two levels. Firstly, the selected clays (Montmorillonite and green Illite) were mainly used previously as heterogeneous catalysts for fatty acid esterification (**Rezende and Pinto, 2016**) and biolubricant synthesis (**Luna et al., 2018**) or as adsorbents for heavy metal removal from waste water (**Gu et al., 2019**); however, they have never been investigated as adsorbents for dry-purification of ethyl biodiesel and biolubricants to the knowledge of the authors. Secondly, ground Indian mustard stems, with and without pyrolysis or carbonization treatment as conducted here, have never been investigated previously for bioproduct purification. Yet agricultural residues have been used successfully as natural adsorbants with or without thermochemical treatment; examples include, but are not limited to: rice husk ash

(Nitièma-Yefanova et al., 2015), virgin banana peel (Banga et al. 2015) or oil palm empty fruit bunch (Ahmad Farid et al., 2017) for biodiesel dry-purification; activated carbon derived from apricot seed kernel (Fadhil, 2017), plantain fruit stem (Ekpete et al., 2017) or virgin peanut hull (Ali et al., 2016) for waste water treatment. More generally, cellulosic biomass can act as an adsorbent in virgin or modified form (Suhas et al., 2016; Sandouqa et al., 2020) and this characteristic is highlighted in this paper.

2. Materials and methods

The flow diagram shown on **Figure 1** depicts the methodology, experimental technics and measured properties that have been selected for characterizing the bioproduct samples and thus optimizing the purification procedure.

2.1. Materials

Solvents and reagents (n-heptane, toluene and citric acid) and chromatographic standards (1-pentanol, methyl heptadecanoate and ethyl oleate) of analytical grade were purchased from Merck, Sigma-Aldrich and Acros Organics.

2.1.1. Production of the crude liquid bioproducts

KOH-based ethanolysis of the Indian mustard seed oil (IMSO) to obtain the crude biofuel (ethyl biodiesel designated as IMSOEEs) was detailed in our previous work (Chen et al., 2019); the main stages being recalled on **Figure 1**. A fraction of these IMSOEEs was then purified by dry-washing (Section 2.4) while the remainder was converted by KOH-based transesterification with 2-ethyl-1-hexanol (2EH), to obtain the crude biolubricant (designated as IMSO2EHes). The details of this second step of conversion are given by Chen et al. (2019) and the dry-purification of the crude IMSO2EHes is described in Section 2.4. Mild operating conditions were selected for the IMSO ethanolysis (35°C, atmospheric pressure, ethanol to IMSO molar ration of 8, 1.1wt% KOH, two-stages separated by addition of recycled glycerol, 50 min) and for the vacuum reactive distillation of the IMSOEEs with 2EH (0.05 bar, 70°C, 2EH to IMSOEE molar ratio of 2, 2wt% KOH, 65 min). Composition of the crude liquid bioproducts (IMSOEEs and IMSO2EHes) both in terms of targeted species and contaminants is given in Results and discussion (**Table 4**).

2.1.2. Production of the solid adsorbents

Indian mustard stems, previously sundried for 2-3 days, were ground and sieved to obtain two classes of particle size; the finest particles ranging from 100 to 710 μm were designated FIMS and the largest ranging from 710 to 1400 μm were designated MIMS. While a fraction of each particle class was used without any further treatment as adsorbents, the remaining fractions were further treated by pyrolysis or carbonization, to produce four additional classes of organic adsorbents; respectively labeled pFIMS, pMIMS, cFIMS and cMIMS. Pyrolysis was conducted in a quartz tubular reactor fed with the FIMS or MIMS and maintained at 500°C for 60 min under a constant flow of nitrogen; passivation of the pyrolyzed material was then achieved with a flow of oxygen diluted in nitrogen during cooling to room temperature. Carbonization was conducted in a muffle furnace maintained at 500°C by placing the FIMS or MIMS in crucibles made of porcelain for 60 min and 8 h, respectively; these crucibles were then removed from the furnace and cooled in air.

The two green clays selected as mineral adsorbents; Montmorillonite (Mt) and Illite, were kindly supplied by EMSPAC France and used after oven drying (110°C for 48 h) without any further treatment.

All prepared adsorbent samples were stored in plastic bottles under dry atmosphere.

2.2. Adsorbent characterization toward determination of “Structure - Adsorption efficiency”

The adsorbent characterization was assessed through average particle size D [3,2] using Laser diffraction, morphology using scanning electron microscopy (SEM), elemental chemical composition by coupling SEM with microanalysis by energy dispersive X-ray spectroscopy (EDS), chemical structure such as bonds and rings using Fourier Transform Infrared spectroscopy (FTIR) and porosity and specific surface area using CO₂ or N₂ adsorption associated with the two-dimensional non-local density functional theory (2D-NLDFT), the Dubinin-Astakhov or the Brunauer-Emmett-Teller (BET) method. The equipment used to collect this information, together with the selected operating conditions, are described in **Table 1**.

2.3. Liquid bioproduct characterization for evaluation of the purification methods

The quality of the biofuel and biolubricant, before and after dry-purification on adsorbent, was evaluated using various analytical methods. Water content was determined by Karl Fischer titration. Triacylglycerides (TGs), diacylglycerides (DGs), monoacylglycerides (MGs), free glycerin, esters (IMSOEEs and IMSO2EHs) and alcohols (ethanol and 2EH) were quantified by gas chromatography with a flame ionization detector (GC-FID). Levels of heavy metals and potassium (resulting from the IMSO extraction stage and the selected catalyst KOH) were ascertained by inductively coupled plasma-atomic emission spectroscopy (ICP-AES). Some functional properties of the final biofuel and biolubricant including acid value, color, density, viscosity, flash point, cloud point, pour point and cold filter plugging point were evaluated following ASTM or ISO standards. The equipment used to collect this information, together with the selected operating conditions are described in [Chen et al. \(2019\)](#) (Appendix A). Nonetheless, higher heating value and oxidation stability of the final biofuel were estimated from [Hong et al. \(2014\)](#) method.

2.4. Purification procedures

The dry-purification was conducted in batch mode within a two-neck round bottom flask equipped with a thermometer ($\pm 0.5^\circ\text{C}$), a polytetrafluoroethylene stir bar and a magnetic stirrer heating system with temperature-control ($\pm 1^\circ\text{C}$). A mixture of 4 wt% adsorbent in crude liquid bioproduct (approximately 45 g, exactly weighed) was maintained under stirring for 20 min following previous methods ([Nitièma-Yefanova et al., 2015, 2017](#)). However, the mixing temperature was set to 35°C for the crude biofuel and to 45°C for the crude biolubricant. The solid/liquid separation was then performed by vacuum filtration over Sartorius™ nitrate membrane filters (pore sizes: $0.2\ \mu\text{m}$). Moreover, the maximum number of treatment cycles (with renewed adsorbent) was fixed at three so that this parameter could be differentiated from the remaining analysis.

The further wet-purification was applied to the crude biolubricant by batch bubble-washing at 25°C and 1 atm, with a 4 wt% citric acid solution in distilled water during the first treatment cycle and with distilled water for the subsequent cycles. To evaluate the benefits of the prior dry-purification, a fraction of the crude biolubricant was treated exclusively by bubble-washing at various operational temperatures and using a larger number of wet-treatment cycles. The washing solution and crude biolubricant, in volume proportions $1/3 - 2/3$, were poured in a separating funnel equipped with a fritted glass cannula connected to an air pump via a control valve ([Chen et al., 2019](#)). Treatment cycles were carried out by

renewing the washing solution (heavy liquid phase) until a constant concentration of potassium was observed following the quantification by Flame Atomic Emission Spectroscopy method described by [Chen et al. \(2019\)](#) (Appendix A). The wet-purification was then finalized by vacuum fractional distillation (0.01 bar max.) ([Chen et al., 2019](#)).

3. Results and discussion

All experiments and analyzes were conducted at least in duplicate (and more frequently to resolve disagreement or inconsistency) and an average value estimated for subsequent analysis and interpretation.

3.1. Adsorbent characterization

3.1.1. Organic adsorbents

The yields of pyrolysis and carbonization (defined as $Y(\text{wt}\%) = (m_i / m_0) \times 100$, with m_i and m_0 the mass of sample before and after thermal treatment) were 28 and 4 ± 1 wt%, respectively, for both FIMS and MIMS regardless of their different particle sizes.

Morphological analysis using SEM revealed a heterogeneous structure for each class of adsorbent (FIMS, MIMS, before and after pyrolysis or carbonization) with some compositional variation in the main elemental components C, O, Ca and K, observed when coupling SEM with microanalysis by EDS (**Figure 2**). Indeed, the ratio Ca/K appears to be higher in the bark than in the core of the Indian mustard stems, with a larger proportion of bark in the MIMS than in the FIMS (**Figure 2b**). This heterogeneity in morphology and composition of the samples remains after thermal treatment, thus increasing the C/O ratio by consumption of oxygen bonds (**Figures 2a1-2c1** and **2a2-2c2**). Indeed, as demonstrated by FTIR analysis, the FIMS are rich in cellulose and hemicellulose (about 40 and 20 wt%, respectively ([De et al., 2018](#))) with hydroxyl O-H and etheric C-O bonds (**Figure 3**).

Observation from SEM of nonporous or macroporous surfaces of FIMS and MIMS with large pores shows quite flat adsorption isotherms with low quantities of N₂ adsorbed (**Figure 4a**). On the other hand, the pFIMS and pMIMS depict accentuated CO₂ adsorption in the low equilibrium relative pressure P/P° values (below 0.01), typical of micro-mesoporous materials (**Figure 4b**) with pore width and pore volume lower than 16 Å and 0.21 cm³/g,

respectively (**Table 2**). From the CO₂ adsorption isotherms, it was possible to determine, for the two samples, the pore size distribution (PSD), the pore volume and the specific surface area by using the 2D-NLDFT method. The Dubinin-Astakhov method, used previously for verification, showed the existence of a heterogeneous microporous distribution where the PSDs from the 2D-NLDFT method present two modes at 4 and 6 Å, together with a more widespread distribution ranging from 8 to 36 Å for pFIMS and 8 to 49 Å for pMIMS (**Figure 5**). Combining these results with the cumulative pore volume curves plotted on **Figure 5**, it can be deduced that around 40 % of the samples contain micropores (pore width < 7 Å) and 60 % mesopores (pore width > 20 Å). Furthermore, as expected, pyrolysis treatment allows the FIMS and MIMS particles to decrease in size while increasing their specific surface area, which should improve the adsorptive capacity of the resulting pFIMS and pMIMS (**Cha et al., 2016**). However, the carbonization treatment not only transformed the FIMS and MIMS into particles of lower size, but also lower specific surface area (**Table 2**). The longer duration of carbonization, applied to the MIMS compared to the FIMS (Section 2.1.2) because of the particle size difference, led to significant changes in textural characteristics. Indeed, while the resulting cMIMS display an adsorption isotherm of type-II (according to IUPAC classification) typical of nonporous or macroporous solids with additionally low N₂ adsorption capacity, the cFIMS show by contrast a hybrid adsorption isotherm of type-I-II, indicating the presence of micropores and meso-macropores (**Figure 4c**). This is confirmed by the PSD determined from the adsorption isotherm showing two modes at 8 and 10 Å (micropores), together with a more widespread distribution ranging from 19 to 488 Å (meso-macropores) (**Figure 5b**). Furthermore, the micropore fraction contributes to 40 % of the CO₂ volume adsorbed by the cFIMS sample (**Figure 5b**). The adsorption isotherms also led to a much lower specific surface area for cMIMS than for the cFIMS; the specific surface area increased in the order: pMIMS > pFIMS > cFIMS > cMIMS (**Table 2**).

3.1.2. Mineral adsorbents

The average chemical composition and physical properties of the two natural clays selected as mineral adsorbents; Montmorillonite (Mt) and Illite, are listed in **Table 3**. The main composition of these clays is silica (SiO₂ ≈ 54 wt%) and alumina (Al₂O₃ ≈ 18 wt%) giving them hygroscopic properties. The main difference between these clays Illite contains titanium dioxide (TiO₂) and the particle size of Mt is almost twice that of Illite particles (**Table 3b**). The both clays exhibit adsorption-desorption isotherms of type-II in the adsorption branch with a hysteresis loop of type-H4 in the desorption branch, indicating the

presence of micropores in non-rigid aggregates of plate-like particles (**Figure 6**) (**Thommes et al., 2015**). Nevertheless, the increase in N₂ adsorbed at high relative pressures P/P° also reveals the occurrence of mesopores. Although the common feature of both clays is the type-H4 loop (i.e. a sharp step-down of the desorption branch located at $P/P^\circ \approx 0.5$ with N₂ at 77 K), the Illite is more adsorbent than Mt (**Figure 6**). This feature is confirmed by the specific surface areas determined by the Dubinin-Astakhov and BET methods; a higher value is obtained for Illite compared to Mt, apparently due to a larger pore volume (**Table 3b**).

3.2. Efficiency of the purification methods and liquid bioproduct characteristics

The purification yields of all liquid bioproducts investigated were defined as $Y(\text{wt}\%) = (m_i / m_0) \times 100$, with m_i and m_0 the mass of sample before and after treatment. The biofuel yields were $95.7 \pm 0.6 \text{ wt}\%$ over Mt or Illite clays; $93 \pm 1 \text{ wt}\%$ over FIMS/MIMS or cFIMS/cMIMS and $87 \pm 1 \text{ wt}\%$ over pFIMS/pMIMS; the decrease observed for the latter materials being partly due to their higher adsorptive capacity (Section 3.1.). The dry-purification biolubricant yields were $81 \pm 2 \text{ wt}\%$ and $86 \pm 1 \text{ wt}\%$ over the mineral and organic adsorbents, respectively and $97 \pm 3 \text{ wt}\%$ for the further wet-purification (including the distillation).

3.2.1. Biofuel characteristics versus adsorbent and dry-purification procedures

Characterization of the biofuel produced before and after dry-purification using the investigated adsorbents and treatment efficiency are reported in **Table 4**. Each of the three cycles of treatment improved biofuel quality, however, the first treatment cycle was by far the most effective. The proposed dry-purification procedure, combined with any adsorbent, produced satisfactory results by concentrating the treated samples in IMSOEEs, while removing most contaminants thus approaching or even satisfying specifications. The exception was water, which was released by all organic adsorbents and likely a consequence of improper sample storage and/or insufficient drying of filtration equipment before use. By contrast, water was adsorbed by both clays thanks due to higher SiO₂ content (Section 3.1.2.). Nevertheless, it is worth highlighting the very good performance of the FIMS and Mt clay in capturing free fatty acids (FFAs). This is very likely due to the O-H hydroxyl groups existing in the structure of these adsorbents (**Figure 3** for the FIMS rich in cellulose; **Gu et al., 2019** for the Mt clay). The Mt clay is also remarkably good at blocking large molecules such as

MGs in its expandable layered lattice (Gu et al., 2019). However, the adsorbents performed poorly for some chemical elements. Indeed, during the dry-purification over FIMS and more significantly over the MIMS, calcium was leached into the filtered biofuel; probably a consequence of the higher concentration of Ca for MIMS. However, this phenomenon was not observed in the thermally treated organic adsorbents. In contrast, potassium was removed effectively by the FIMS and MIMS, together with both clays, but very poorly by the pFIMS/pMIMS and the cFIMS/cMIMS; likely a consequence of thermal degradation of their O-H bonds during the pyrolysis or carbonization process (Section 3.1.1). It should be noted that the K capture by FIMS and MIMS and the two clays, may explain in part the water released in the treated biofuel according to:

$\text{Cellulose-OH} + \text{KOH} \rightarrow \text{Cellulose-OK} + \text{H}_2\text{O}$ for the FIMS and MIMS, and

$\text{Clay-OH} + \text{KOH} \rightarrow \text{Clay-OK} + \text{H}_2\text{O}$ for the Mt or Illite,

with formation of alcoholate of potassium on the adsorbent and partial release of water in the biofuel.

The best performing adsorbents were clearly FIMS and the Mt clay. Indeed, the Mt clay was identified as an excellent adsorbent, particularly for FFAs, water, MGs and IMSOEEs (Table 4). On the other hand, FIMS were identified as a cost-effective option for the biorefinery concept using Indian mustard residue. They were transformed by a simple mechanical process prior to IMSO conversion and can be reused (with or without thermal treatment) as a soil corrective due to their biodegradable organic and potassium content.

Although dry-purification over FIMS and the two clays did not produce biofuel that meets specifications in terms of IMSOEEs and contaminants (Table 4), valuable functional properties were observed in the three purified samples of biodiesel (Table 5). The biodiesel samples were labelled Biofuel-FIMS-3, Biofuel-Mt-3, Biofuel-Illite-3; referring to the liquid bioproduct, the adsorbent and the number of cycles of treatment. Thus, it would be worth conducting thermal and emission analyses to study these fuels further.

3.2.2. *Biolubricant characteristics versus adsorbent and purification procedures*

Based on the biofuel dry-purification results, the FIMS and the Mt clay were selected as adsorbents to study the biolubricants using a single cycle of dry-purification. All biolubricant samples are therefore designated as: Biolub-Adsorbent- further wet-purification (W) and distillation (D). The characterization of the biolubricant before and after purification is shown in Table 6. The FIMS and to a larger extent the Mt clay removed a large part of the

K remaining in the reaction mixture after the KOH-catalyzed transesterification of the IMSOEEs with 2EH. The lower capacity of these adsorbents to remove K (-62 and -75 wt% removal for FIMS and Mt, respectively) compared to biofuel purification (-100 wt% for both adsorbents) is likely due to the higher viscosity of the biolubricant which is made of larger molecules. Moreover, the micro-mesoporous Mt clay (Section 3.1.2) captures in part some organic contaminants, small and large molecules, including excess ethanol and 2EH and non-converted IMSOEEs, while the macroporous FIMS show a significant adsorptive capacity specifically for non-converted IMSOEEs.

The further wet-purification of the biolubricant by bubble-washing (first with 4 wt% citric acid solution and then with distilled water) eliminated almost all the remaining K. The subsequent vacuum distillation finalized the biolubricant drying and simultaneously removed the remaining 2EH (forming a heterogeneous azeotrope with water) while concentrating the IMSO2EHs. Nonetheless, the vacuum reached with the equipment used (minimum operational pressure of 0.01 bar) was not enough to remove the non-converted IMSOEEs.

The benefit of a preliminary dry-purification compared to an exclusive wet-purification was a decrease in the number of wet-treatment cycles and associated production of waste water and reduced biolubricant production time (**Figure 7**). Indeed, only 5 washing cycles are required to remove almost all potassium from the biolubricant previously purified over FIMS or Mt (**Figures 7a-7b**), compared to 13 washing cycles for the exclusive wet-purification (**Figure 7c₁**). This results in a reduction of the wet-purification time from 250 min to 50 min. Thus, the proposed hybrid purification saves water and time with an 80 and 20% reduction, respectively. Moreover, as shown by **Figure 7c₂**, the effectiveness of bubble-washing with citric acid solution was better at 30-35°C than 65°C. In addition, 2EH remaining in the biolubricant has a very low solubility in water at 25°C under atmospheric pressure (880 mg/L) and for this reason the wet-purification of both Biolub-FIMS and Biolub-Mt was conducted at 25°C.

Functional properties and composition in IMSO2EHs of the purified biolubricant samples (Biolub-FIMS-W&D and Biolub-Mt-W&D) are presented in **Table 5**. The final products showed satisfactory behavior as biolubricants, particularly as metalworking fluids, in terms of acid value, density, viscosity, and color (**McNutt and He, 2016; Zheng et al., 2018**). The difference in color between the biolubricants prepared in this work and that selected as the reference (Biolub-Ref) (**Valtris, 2019**), comes from the parent oil (orange for the IMSO and pale yellow for the rapeseed oil used in the production of Biolub-Ref.). Nonetheless, because no tribological tests (for analyzing lubricity, friction and wear behaviors) could be

performed in this work, the final Biolub-products should be reasonably considered as potential biolubricants, pending such complementary testing. In addition, fewer FFAs were removed by FIMS than by Mt clay as (confirmed by the higher acid value of Biolub-FIMS-W&D). Moreover, bubble-washing with a less concentrated citric acid solution at lower temperature would decrease the high acid value, depicted by Biolub-W&D, without a significant loss of efficiency. The citric acid concentration should be optimized to remove the catalyst from the biolubricant by formation of potassium citrate in the water phase. This precaution would avoid formation of excess soluble citric acid in the biolubricant phase (Chen et al., 2019). The existence of citric acid and glucosinolates following bubble-washing shows that these are less efficiently removed than by dry-purification over FIMS or Mt, and would explain the low IMSO2EHE content in Biolub-W&D (88 wt%, Table 6). These glucosinolates, naturally present in the departure IMSO, also deplete the glyceride pool that can be converted into esters (IMSOEEs or IMSO2EHEs). Hence, a pre-treatment of the departure IMSO prior to any transesterification would enhance ester content thus ensuring that the produced biofuel and biolubricant strictly conform to specifications. Nonetheless, citric acid enhanced oxidation stability of both biolubricants and biodiesel (Sharma and Biresaw, 2016; Serrano et al., 2013) and this compensated the rather high ratio of polyunsaturated esters compared to monounsaturates of the obtained liquid bioproducts (ratio of ≈ 0.8 %), thus ensuring good thermal-oxidative stability (Chan et al., 2018).

Lastly, the behavior of all the materials tested in this work illustrates the two complementary criteria, enthalpic and entropic, governing the performance of an adsorbent. The entropic criterion offering a physical selectivity by steric hinderance (induced by a high specific surface area making accessible adsorption sites of various width, ranging from micropores to macropores) is well illustrated by the Mt clay. By contrast, the enthalpic criterion offering a chemical selectivity by functional groups (located inside the adsorbent pores that help capturing specific species) is rather illustrated by the FIMS. Thus, an alternative to preparing a more effective adsorbent would be to formulate a mixture of FIMS and Mt clay in appropriate proportions to combine the most desired properties of both materials.

3.3. Potential Indian mustard biorefinery aspects in tune with a green circular economy

This section aims at highlighting a potential biorefinery system focused on Indian mustard contributing to a green circular economy that would benefit both farmers and

consumers in the respect of environment. The objective is to illustrate that within such a system, farmers would gain in energy security and flexibility by on-farm production of biofuel, biolubricants and other bioproducts, while ensuring healthy food security and offering job opportunities, the whole with reduced chemical and energy inputs and minimized waste effluents. This aspect of the work is all the more helpful that very few biorefineries generating ethyl biodiesel and biolubricants among the biobased product streams have been investigated in the literature (Ubando et al., 2020). The case study carried out by Rapp (2018) on the value of Indian mustard in cereal and legume crop sequences in New South Wales (NSW) of Australia is taken as departure (area: 5 ha; period: 3 years, from 2013 to 2015; amount of seeds planted (kg/ha): 2). Indian mustard is considered there for its biofumigation properties. In the potential biorefinery presented here, the phytoremediation aspect of Indian mustard (Raj et al., 2020) was also included in a hypothetical scenario.

3.3.1. *Keyword network of the Indian mustard biorefinery*

The main keyword network of the biorefinery focused on Indian mustard is shown **Figure 8**. The description is non-exhaustive and gives only an overview restricted to the applications focused by the present work. All the parts of the plant, i.e. seeds, stems and roots contribute to the network whatever Indian mustard is used for biofumigation or phytoremediation. Nonetheless in this later case, the seeds, and thus the resulting oil and meal, cannot be used for human and animal consumption but only for non-edible applications such as production of biofuels (ethyl biodiesel) and bioproducts (biolubricants, bioplasticizers...) Other directions could be adopted depending on the results obtained from studies aimed at determining which parts of the mustard plant accumulate metals.

After extracting the oil from Indian mustard seeds, the highly valued glucosinolates (GLSs) are removed from the protein-rich meal which can then be safely used for animal feed. In fact, GLSs, which are among the metabolites responsible for the biofumigation properties of Indian mustard, have benefits for human and animal health, provided they are included in diet in controlled doses (Rapp, 2018). Hence, apart from their application as biopesticides (Hebert et al., 2020), GLSs may also be used in manufacturing pharmaceuticals and veterinary products (Rapp, 2018). As illustration, sinigrin and gluconasturtiin have revealed anti-cancer, with additional antibacterial, antifungal, antioxidant, anti-inflammatory activities for sinigrin (Mazumder et al., 2016). Depending on its nutritional quality, Indian mustard oil is either intended for human food where it is sought after for its spicy taste (route A, **Figure 8**), or oriented towards the production of ethyl biodiesel and biolubricants showing

better lubricating properties due to high erucic acid ([Chen et al., 2019](#)) (route A&B, **Figure 8**). Despite the recycling of crude glycerol in the reaction medium to improve the biodiesel yield, an excess of residual glycerol is formed. This one, together with the wastewater resulting from the bubble washing of the biolubricants, are sent to a dedicated biodigester where they are converted into biohydrogen and bioethanol ([Patil et al. 2016](#)). After purification, bioethanol thus produced can be used to feed the ethyl biodiesel production unit. The Indian mustard stems used after dry-purification of the liquid bioproducts (ethyl biodiesel and biolubricants), as well as the roots, are directed to a biological or a thermal cogeneration unit for being converted into biogas, biofertilizers, heat and power. The Montmorillonite clay is however sent exclusively to the thermal cogeneration unit where it is regenerated for being reused as adsorbent in the dry-purification of the liquid bioproducts (ethyl biodiesel and biolubricants).

Thus, the biorefinery focused on Indian mustard as described here integrates various conversion technologies (chemical, thermochemical, biochemical and combustion) to efficiently produce sustainable food, feed and biobased product streams such as biofuels, bioenergy and other high-valued bioproducts (biofertilizers, biopesticides, pharmaceuticals, veterinary products). Moreover, various biomass sources are converted by technologies in tune with process intensification (such reactive distillation for biolubricants production), while reusing byproducts in the network to minimize resource consumption and waste generation.

Lastly, Indian mustard acting as a break crop, with the resultant seed and biomass used for industrial purposes, does not compete with food crops, but rather enhances food production through biofumigation and the application of biofertilizers. Hence, Indian mustard cultivation does not create indirect land use change, but enhances arable land use. Ethyl biodiesel produced from mustard oil (mainly with high levels of erucic acid) is a by-product that allows to regulate both the income of farmers regardless of climatic conditions and the price of mustard oil on the food market in the event of overproduction, while ensuring energy security. Moreover, [Oláb et al. \(2017\)](#) showed that the main driver for food price fluctuation is the oil price shock but is not the consequence of a rising and competitive biofuel production. Also, still according to the work by [Oláb et al. \(2017\)](#), Indian mustard should induce greenhouse gas (GHG) emission savings because the protein-rich meal generated as co-product and used as feed reduces land use and thus the demand for chemical inputs in the feed production.

3.3.2. *Related environmental, economic and social aspects in further details*

Beside its implication for biofumigation and as biofertilizer, Indian mustard requires very little irrigation. These features minimize its environmental footprint when considering that fertilizer production induces notable energy consumption and GHG emissions and that water is a finite resource. Also, Indian mustard can adapt to climate change without being invasive and can therefore be grown with respect for biodiversity and the surrounding ecosystem.

Regarding the costs and income from Indian mustard sales at the Australian farm level, the gross margin budget estimated by the [NSW Department of Primary Industries](#) is about 251 AUD/ha resulting from a total income of 589 AUD/ha (for an Indian mustard yield of 1.30 ton/ha at 460 AUD/ha) and total variable costs (for the sowing, fertilizer, herbicide, insecticide, contract harvesting, ...) of 347 AUD/ha. Although dating 2012, these estimations still remains very close to 2020 prices. This gross margin was estimated on an open loop market; the growers operating under closed loop market, i.e. supplying a processing plant directly with no delivery costs, at a contracted price of 750 AUD/ton, the gross margin reaches in that case 975 AUD/ha.

The revenue projection for Indian mustard oil over 5 years (2021-2026), from plantation to processing plant including the benefits of biofumigation, is estimated to be approximately AUD 119 million, the savings from soil biofumigation and improved cereal yield contributing to 67%, the value of premium mustard oil to 22% and the value of seeds to 11% (**Table 7**) ([Rapp and Kemp, 2020](#)). The costs involved in converting mustard seeds to premium oil were not factored into these estimates because it was assumed that the reference method by first cold pressing (mechanical process squeezing the seeds at low to ambient temperatures to remove the oil without using chemicals) was selected by default. The remaining factor to consider is then the costs involved in converting Indian mustard oil into biofuel and other biobased products (scenarios concerned: mustard oil with high erucic acid levels or mustard used for phytoremediation). This conversion method should be efficient, environmentally-friendly and low-cost to be beneficial.

Table 8 ([Coniglio et al., 2013](#); [Coniglio et al., 2014](#); [Nitièma-Yefanova et al., 2016](#); [Kargbo et al., 2021](#)) shows the main characteristics of the methods used to produce biofuels similar to petrodiesel from various biomass resources. For all these conversion methods, the key challenge actually lies in the pretreatment step of the raw material which is quite complex for the lignocellulosic and algal biomass, the cell walls of which are recalcitrant ([Sakaran et al., 2020](#)). Moreover, thermal conversion of lignocellulosic or algal biomass leads to drop-in

fuels, i.e. hydrocarbons very similar to fossil fuels, but at a high energy and processing cost. On the other hand, the transesterification by alkaline catalysis of vegetable oils with a short alcohol (generally methanol) leading to biodiesel is efficient and inexpensive, and becomes even more environmentally-friendly by operating with ethanol (instead of methanol), at ambient temperature (instead of 65 °C), and under dry purification (instead of the wet purification), as was done in the present work. Similarly, as illustrated by **Table 9 (Syahir et al., 2017; Chen et al., 2019)**, production of biolubricants by transesterification is an efficient and cheap route compared to the other methods, particularly by adopting the ethyl biodiesel as reactional intermediary and high vacuum to decrease the reaction temperature (achieved using an ejector at industrial scale). Furthermore, this route does not require any harmful reagents or rare catalysts, and offers the possibility of using a wide variety of long-chain alcohols to obtain biolubricants with variable properties.

Using the BioCube technology (Canada) based on transesterification, the production costs for biodiesel in AUD/Litre fall to 0.70 from used cooking oil and to 0.65 from Indian mustard oil (**Rapp, 2018**). At this stage, biodiesel starts to compete with petrodiesel (which terminal gate price in Australia is 0.98 AUD/Litre) when considering the benefits induced by the conversion of a non-edible oil obtained from an Indian mustard which would have been used, either for phytoremediation (oil potentially containing traces of metals), or for biofumigation (but in wet/cold climatic conditions potentially leading to an erucic acid rich oil) and the extraction of glucosinolates from the mustard meal (current value of sinigrin which production can reach 90 kg/ha of mustard crop: 140 AUD/100 mg) (**Rapp, 2018**). Although the production costs associated with the conversion route developed in the present work have not been estimated, operating at ambient temperature with ethanol that may be obtained from agricultural residues should at least result in similar (if not lower) production costs. Moreover, ethyl biodiesel has better biodegradability, higher flash point, improved cold-flow properties and oxidation stability, and lower emissions of NO_x, CO, and ultrafine particles than methyl biodiesel (**Coniglio et al., 2013**).

Thus, in addition to environmental and economic benefits previously mentioned, such industrialization based on an adaptive agriculture system should boost the education of very young people to adults, at the same time as the creation of new jobs and the resilience of existing ones. Indeed, farmers and their employees, as well as their family circles, will first have to update their skills and knowledge. However, this investment will offer them the possibility of adapting their production without loss of income according to climatic and economic conditions (supply and demand on the markets), and of widening their field of

action by producing various on-farm bioproducts (ethyl biodiesel, biolubricants), in addition to food, feed, agricultural and veterinary products. Such a context should guarantee the sustainability of the biorefinery focused on Indian mustard within a green circular economy, in accordance with [Urbancová \(2013\)](#) and [Maroušek et al. \(2015\)](#) who identified that knowledge is the keystone in the process of innovation and that both innovation and knowledge offer to improve the overall competitiveness of any organization of a country.

3.3.3. Future research

Scaling up, from the lab to the pilot scale, the Indian mustard oil conversion process to final bioproducts (ethyl biodiesel and biolubricants) is a key stage to demonstrate the viability of the process on the semi-industrial scale. Indeed, experiments carried out with this pilot would not only be aimed at searching for optimal operating conditions leading to maximum bioproduct yields and minimum energy and matter demands. Information obtained from these experiments, including meaningful material and energy balances, would also be used to validate the estimates obtained by process simulation. Actually, reliability of estimates given by any simulator depends on the theoretical models implemented in the software for describing the thermodynamic, kinetic and transport phenomena involved in the various unit operations of the process (Coniglio et al., 2014). While theoretical models are rather well documented for ethyl biodiesel, the same would not apply for biolubricants. The required experimental kinetic data could be generated from the continuous reactive-distillation unit of the pilot; however, experimental phase equilibria studies should be carried out by ebulliometry for updating the required thermodynamic model (Muhammad et al., 2017). Such an approach should secure the reliability of the simulations and optimizations carried out on the pilot, together with the related life cycle assessment aimed at diagnosing the opportunity of extrapolating the pilot at the most convenient scale (semi-industrial or smaller). From the diagnosis made at this stage, all the required tools would be ready for designing safely the Indian mustard conversion unit at the desired scale.

Nonetheless, regarding dry purification, the transfer from the laboratory-scale batch mode to the pilot-scale continuous mode requires a techno-economic analysis to be performed with particular attention. Indeed, although the general rule of technology transfer is that cost reduction up to one third may be expected if the technology is implemented on a commercial scale, exceptions may be observed if technological revisions must be made to compensate for performance losses due to scale changes (Maroušek, 2015). Using a combination of FIMS and Mt clay to enhance the performance of the resultant adsorbent may mitigate the effect of scale change.

Moreover, when Indian mustard is used for phytoremediation or when Indian mustard oil is expected to be high in erucic acid, a method involving lower cost than cold pressing dedicated to produce edible oil of high nutritional quality should be selected. High pressure shock waves (50-60 MPa) caused by high voltage electrical discharges (HVED, 3.5 kV) showed very efficient in disintegrating plant cells. Combined with previous pretreatment (grinding then maceration in excess methanol (Maroušek, 2012) or gasification with small

amounts of CO₂ (Maroušek, 2014)), HEVD technology led to significant improvement of oil extraction (up to 93%) for various oilseeds, such as *Jatropha curcas* L. (Maroušek, 2012) or rapeseed (Maroušek, 2013a). HEVD technology could be tested on Indian mustard seeds with however adjustment of the pretreatments to allow recovery of the high added value GLSs from the meal obtained after oil extraction. Indeed, myrosinase, an enzyme naturally found in Indian mustard seeds and compartmentalized in cells in close proximity to GLSs, is responsible for hydrolyzing GLSs upon plant tissue disruption (Doheny-Adams et al., 2017). Hence, myrosinase should be inactivated before any mustard seeds processing. A proposal for Indian mustard oil extraction could be to start by heating the seeds to 90°C in order to inactivate almost all of the myrosinase without affecting the oil, GLSs and proteins content and quality (Hebert et al., 2020). The seeds, after CO₂ gasification, would then be treated by HEVD in ethanol excess (replacing methanol) acting both as a liquid carrier for the pressure shock waves and as a green solvent increasing the mustard oil extraction efficiency. After filtration to separate the meal, the remaining ethanol could then be used for oil conversion into ethyl biodiesel and then biolubricants, while the meal could be ground and then treated by HVED in excess ethanol to obtain separately the GLSs and a meal rich in proteins suitable for animal feeding (Hebert et al., 2020).

In addition, it would be essential to research which parts of the plant capture the greatest amounts of metals and whether this capture is selective in order to define the most appropriate use of seeds (and thus of the extracted oil and remaining meal), leaves, stems and roots. Meanwhile, for dry purification, Indian mustard stems grown on non-contaminated soil will be used as an adsorbent until further studies are conducted to investigate the potential leaching of contaminated stems into treated bioproducts.

Lastly, prior being directed to the biodigester, the used FIMS could be subjected to pressure shock waves, with preliminary treatment by hot-maceration then steam-explosion, for enhancing biogas production (Maroušek, 2013b). Preliminary studies need to be carried out at the Lab scale to confirm this assumption.

4. Conclusions

Among the various natural adsorbents investigated in this work, Montmorillonite clay and finely ground Indian mustard stems without further pyrolysis or carbonization treatment,

performed best. Combined with the selected dry-purification procedure (35-45°C, 20 min, single treatment cycle), impurities were effectively removed from the produced ethyl biodiesel including residual glycerides, free glycerin, water, catalyst and metals introduced during the oil extraction by Indian mustard seed crushing.

The produced ethyl biodiesel had a satisfactory ester content (95.8 wt %) and subsequently met the basic biodiesel properties of acid value, color, density, viscosity, flash point, pour point, cloud point, cold filter plugging point, higher heating value and oxidation stability.

A single cycle of dry-purification over the Montmorillonite clay or the finely ground Indian mustard stems optimized biolubricant quantity and quality, but further purification by bubble-washing (using citric acid) and vacuum distillation (less than 0.01 bar) was required to obtain a product with high ester content (92.5 wt%) that exhibited good basic properties of density, viscosity and color. Such a procedure combining dry-purification with subsequent bubble-washing and vacuum distillation offers the advantage of reduced water consumption compared to the wet purification usually carried out by industry. Nonetheless, in the absence of tribology tests, the products obtained should reasonably be considered as potential biolubricants.

The used Indian mustard stem adsorbent could then be converted inside a cogeneration unit to produce heat, power and biofertilizers. Hence, this work tends to confirm that Indian mustard can be implemented in an integrated biorefinery system contributing to a green circular economy, with positive environmental, economic and social impacts.

Acknowledgments

The authors are very appreciative to Emilien Girot, Frédéric Roze, and Jean-François Remy for their technical support (members of Université de Lorraine - Ecole Nationale Supérieure des Industries Chimiques de Nancy, Laboratoire Réactions et Génie des Procédés UMR CNRS 7274, 54001 Nancy Cedex, France).

References

Ahmad Farid, M.A, Hassan, M.A., Taufiq-Yap, Y.H., Shirai, Y., Hasan, M.Y., Zakaria, M.R., 2017. Waterless purification using oil palm biomass-derived bioadsorbent improved the

- quality of biodiesel from waste cooking oil, *Journal of Cleaner Production* 165, 262-272. <http://dx.doi.org/10.1016/j.jclepro.2017.07.136>.
- Ali, R.M., Hamad, H.A., Hussein, M.M., Malash, G.F., 2016. Potential of using green adsorbent of heavy metal removal from aqueous solutions: Adsorption kinetics, isotherm, thermodynamic, mechanism and economic analysis. *Ecological Engineering* 91, 317-332. <http://dx.doi.org/10.1016/j.ecoleng.2016.03.015>.
- Banga, S., Varshney, P.K., Kumar, N., 2015. Purification of *Jatropha curcas* based biodiesel by dry washing, using banana peel and mushroom powder as natural adsorbents. *Biofuels* 6, 261-267. <http://dx.doi.org/10.1080/17597269.2015.1092101>.
- Cha, J.S., Park, S.H., Jung, S.C., Ryu, C., Jeon, J.K., Shin, M.C., Park, Y.K., 2016. Production and utilization of biochar: A review. *Journal of Industrial and Engineering Chemistry*, 40 1–15. <http://dx.doi.org/10.1016/j.jiec.2016.06.002>.
- Chan, C.H., Tang, S.W., Mohd, N.K., Lim, W.H., Yeong, S.K., Idris, Z., 2018. Tribological behavior of biolubricant base stocks and additives. *Renewable and Sustainable Energy Review* 93, 145-157. <https://doi.org/10.1016/j.rser.2018.05.024>.
- Chen, J., Bian, X., Rapp, G., Lang, J., Montoya, A., Trethowan, R., Bouyssiere, B., Portha, J-F. Jaubert, J.-N., Peter Pratt, P., Coniglio, L., 2019. From ethyl biodiesel to biolubricants: Options for an Indian mustard integrated biorefinery toward a green and circular economy, 137, 597-614. <https://doi.org/10.1016/j.indcrop.2019.04.041>.
- Coniglio, L., Bennadji, H., Glaude, P.A., Herbinet, O., Billaud, F., 2013. Combustion chemical kinetics of biodiesel and related compounds (methyl and ethyl esters): Experiments and modeling Advances and future refinements. *Progress in Energy and Combustion Science* 39, 340-382. <http://dx.doi.org/10.1016/j.pecs.2013.03.002>.
- Coniglio, L., Coutinho, J.A.P., Clavier, J.Y., Jolibert, F., Jose, J., Mokbel, I., Pillot, D., Pons, M.N., Sergent, M., Tschamber, V., 2014. Biodiesel via supercritical ethanolysis within a global analysis “feedstocks-conversion-engine” for a sustainable fuel alternative. *Progress in Energy and Combustion Science* 43, 1-35. <http://dx.doi.org/10.1016/j.pecs.2014.03.001>.
- De, S., Bandyopadhyay, S., Assadi, M., Mukherjee, D.A. 2018. Sustainable energy technology and policies: a transformational journey, Vol. 1, Book series: Green energy and technology, Ed. Springer, 233 Spring street, New-York, NY 10013, United States, pp. 1-450. <https://doi.org/10.1007/978-981-10-7188-1>.

- Doheny-Adams, T., Redeker, K., Kittipol, V., Bancroft, I., Hartley, S.E., 2017. Development of an efficient glucosinolates extraction method. *Plant Methods* 13, 1-17. DOI [10.1186/s13007-017-0164-8](https://doi.org/10.1186/s13007-017-0164-8).
- EMSPAC, Mons, France, 2019. Private communication.
- Ekpete, O.A., Marcus, A.C., Osi, V., 2017. Preparation and Characterization of Activated Carbon Obtained from Plantain (*Musa paradisiaca*) Fruit Stem. *Journal of Chemistry* 2017, 1-6. <https://doi.org/10.1155/2017/8635615>.
- Fadhil, A.B., 2017. Evaluation of apricot (*Prunus armeniaca L.*) seed kernel as a potential feedstock for the production of liquid bio-fuels and activated carbons. *Energy Conversion and Management* 133, 307-317. <http://dx.doi.org/10.1016/j.enconman.2016.12.014>.
- Feng, Z., Odelius, K., Rajarao, G.K., Hakkarainen, M., 2018. Microwave carbonized cellulose for trace pharmaceutical adsorption. *Chemical Engineering Journal* 346, 557-566. <https://doi.org/10.1016/j.cej.2018.04.014>.
- Gu, S., Kang, X., Wang, L., Lichtfouse, E., Wang, C., 2019. Clay mineral adsorbents for heavy metal removal from wastewater: a review. *Environmental Chemistry Letters* 2019, 17, 629–654. <https://doi.org/10.1007/s10311-018-0813-9>.
- Hossain, M.A., Iqbal, M.A.M., Julkapli, N.M., San Kong, P., Ching, J.J., Lee, H.V., 2018. Development of catalyst complexes for upgrading biomass into ester-based biolubricants for automotive applications: a review. *The Royal Society of Chemistry Advances* 8, 5559-5577. <https://doi.org/10.1039/c7ra11824d>.
- Hong, I.K., Jeon, S.G., Lee, S.B., 2014. Prediction of biodiesel fuel properties from fatty acid alkyl ester. *Journal of Industrial and Engineering Chemistry* 20, 2348-2353. <https://doi.org/10.1016/j.jiec.2013.10.011>.
- Luna, F.M.T, Cecilia, JA., Saboya, R.M.A., Barrera, D., Sapag, K., Rodríguez-Castellón, E., Cavalcante, C.L., 2018. Natural and Modified Montmorillonite Clays as Catalysts for Synthesis of Biolubricants. *Materials* 11, 1764-1782. <http://doi.org/10.3390/ma11091764>.
- Kargbo, H., Harris, J.S., Phan, A.N., 2021. “Drop-in” fuel production from biomass: Critical review on techno-economic feasibility and sustainability. *Renewable and Sustainable Energy Reviews* 135, 110168. <https://doi.org/10.1016/j.rser.2020.110168>.
- Kirkegaard, J.A., Sarwar, M., 1999. Glucosinolate profiles of Australian canola (*Brassica napus annua L.*) and Indian mustard (*Brassica juncea L.*) cultivars: implications for

- biofumigation. *Australian Journal of Agricultural Research* 50, 315-324. <https://doi.org/10.1071/A98124>.
- Maroušek, J., 2013a. Use of continuous pressure shockwaves apparatus in rapeseed oil processing. *Clean Technology Environment Policy* 15, 721-725. DOI 10.1007/s10098-012-0549-3.
- Maroušek, J., 2013b. Prospects in straw disintegration for biogas production. *Environmental Science and Pollution Research* 20, 7268-7274. DOI 10.1007/s11356-013-1736-4.
- Maroušek, J., 2014. Novel technique to enhance the disintegration effect of the pressure waves on oilseeds. *Industrial Crops and Products* 53, 1-5. <http://dx.doi.org/10.1016/j.indcrop.2013.11.048>.
- Maroušek, J., 2015. Economic analysis of the pressure shockwave disintegration process. *International Journal of Green Energy* 12, 132-1235. <https://doi.org/10.1080/15435075.2014.895740>.
- Maroušek, J., Itoh, S., Higa, O., Kondo, Y., Ueno, M., Suwa, R., Komiya, Y., Tominaga, J., Kawamitsu, Y., 2012. The use of underwater high-voltage discharges to improve the efficiency of *Jatropha curcas* L. biodiesel production. *Biotechnology and Applied Biochemistry* 59, 451-456. DOI 10.1002/bab.1045.
- Maroušek, J., Myšková, K., Žák, J., 2015. Managing environmental innovation: Case study on biorefinery concept. *Revista Técnica de la Facultad de Ingeniería Universidad del Zulia* 38, 216 - 220. ISSN 0254-0770.
- McNutt, J., He, Q.S., 2016. Development of biolubricants from vegetable oils via chemical modification. *Journal of Industrial and Engineering Chemistry* 36, 1-12. <http://dx.doi.org/10.1016/j.jiec.2016.02.008>.
- Muhammad, F., Oliveira, M.B., Pignat, P., Jaubert, J.N., Pinho, S.P., Lucie Coniglio, L. 2017. Phase equilibrium data and modeling of ethylic biodiesel, with application to a non-edible vegetable oil 203, 633-641. <http://dx.doi.org/10.1016/j.fuel.2017.05.007>.
- Mazumder, A., Dwivedi, A., du Plessis, J., 2016. Sinigrin and Its Therapeutic Benefits. *Molecules* 21, 416. <https://doi.org/10.3390/molecules21040416>.
- Ngala, B.M., Haydock, P.P.J., Woods, S., Back, M.A., 2015. Biofumigation with *Brassica juncea*, *Raphanus sativus* and *Eruca sativa* for the management of field populations of the potato cyst nematode *Globodera pallida*. *Pest Management Science* 71, 759-769. <https://doi.org/10.1002/ps.3849>.
- Nitiéma-Yefanova, S., Coniglio, L., Schneider, R., Nébié, R.H.C., Bonzi-Coulibaly, Y.L., 2016. Ethyl biodiesel production from non-edible oils of *Balanites aegyptiaca*,

- Azadirachta indica*, and *Jatropha curcas* seeds – Laboratory scale development. *Renew. Energy* 96, 881-890. <http://dx.doi.org/10.1016/j.renene.2016.04.100>.
- Nitièma-Yefanova, S., Richard, R., Thiebaud-Roux, S., Bouyssiere, B., Bonzi-Coulibaly, Y.L., Nébié, R.H., Mozet, K., Coniglio, L., 2015. Dry-purification by natural adsorbents of ethyl biodiesels derived from nonedible oils. *Energy and Fuels* 29, 150-159. <https://doi.org/10.1021/ef501365u>.
- Nitièma-Yefanova, S., Tschamber, V., Richard, R., Thiebaud-Roux, S., Bouyssiere, B., Bonzi-Coulibaly, Y.L., Nébié, R.H.C., Coniglio, L., 2017. Ethyl biodiesels derived from non-edible oils within the biorefinery concept – Pilot scale production & engine emissions. *Renewable Energy* 109, 634-645. <http://dx.doi.org/10.1016/j.renene.2017.03.058>.
- NSW Department of Primary Industries, DRYLAND JUNCEA CANOLA (2012), Farm Enterprise Budget Series - North West NSW.
- Oláh., J., Lengyel, P., Balogh, P., Harangi-Rákos, M., Popp, J. 2017. The role of biofuels in food commodity prices volatility and land use. *Journal of Competitiveness* 9, 81-93. <https://doi.org/10.7441/joc.2017.04.06>.
- Raj, D., Kumar, A., Maiti, S.K., 2020. *Brassica juncea* (L.) Czern. (Indian mustard): a putative plant species to facilitate the phytoremediation of mercury contaminated soils. *International Journal of Phytoremediation*. 22, 733-744. <https://doi.org/10.1080/15226514.2019.1708861>.
- Rapp, G., 2018. The value of Indian mustard in cereal and legume crop sequences in northwest NSW. Master Thesis, University of Sydney, Australia. <http://hdl.handle.net/2123/18504>.
- Rapp, G., Kemp, A., 2020. The revenue projection for Indian mustard oil over 5 years (2021-2026) from planting to processing plant (unpublished). Private communication.
- Rezende, M.J.C., Pinto, A.C., 2016. Esterification of fatty acids using acid-activated Brazilian smectite natural clay as a catalyst. *Renewable Energy* 92, 171-177. <http://dx.doi.org/10.1016/j.renene.2016.02.004>.
- Sankaran, R., Parra Cruz, R.A., Pakalapati, H., Show, P.L., Ling, T.C., Chen, W.H., Tao, Y., 2020. Recent advances in the pretreatment of microalgal and lignocellulosic biomass: A comprehensive review. *Bioresource Technology* 298, 122476. <https://doi.org/10.1016/j.biortech.2019.122476>.

- Sandouqa, A., Al-Shannag, M., Al-Hamamre, Z., 2020. Biodiesel purification using biomass-based adsorbent manufactured from delignified olive cake residues. *Renewable Energy* 151, 103-117. <https://doi.org/10.1016/j.renene.2019.11.009>.
- Serrano, M, Bouaid, A., Martinez, M., Araci, J., 2013. Oxidation stability of biodiesel from different feedstocks: Influence of commercial additives and purification step. *Fuel* 113, 50-58. <http://dx.doi.org/10.1016/j.fuel.2013.05.078>.
- Sharma, B.K., Biresaw, G., 2016. Environmentally friendly and biobased lubricants, First ed. CRC Press Taylor & Francis Group. ISBN 9781482232028.
- Suhas, Gupta, V.K., Carrott, P.J.M., Singh, R., Chaudhary, M., Kushwaha, S., 2016. Cellulose: A review as natural, modified and activated carbon adsorbent. *Bioresource Technology* 216, 1066-1076. <http://dx.doi.org/10.1016/j.biortech.2016.05.106>.
- Syahir, A.Z., Zulkifli, N.W.M., Masjuki, H.H., Kalam, M.A., Alabdulkarem, A., Gulzar, M., Khuong, L.S., Harith, M.H., 2017. A review on bio-based lubricants and their applications. *Journal of Cleaner Production* 168, 997-1016. <http://dx.doi.org/10.1016/j.jclepro.2017.09.106>.
- Thommes, M., Kaneko, K., Neimark, A.V., Oliver, J.P., Rodríguez-Reinoso, F., Rouquerol, J., Sing, K.S.W. 2015. Physisorption of gases, with special reference to the evaluation of surface area and pore size distribution (IUPAC Technical Report). *Pure and Applied Chemistry* 87, 1051–1069. <https://doi.org/10.1515/pac-2014-1117>.
- Ubando, A.T., Felix, C.B., Chen, W.S., 2020. Biorefineries in circular bioeconomy: A comprehensive review. *Bioresource Technology* 299, 122585. <https://doi.org/10.1016/j.biortech.2019.122585>.
- Urbancová, H. 2013. Competitive advantage achievement through innovation and knowledge. *Journal of Competitiveness* 5, 82-96. <https://doi.org/10.7441/joc.2013.01.06>.
- Valtris Enterprises France, Verdun, France, 2019, Private communication.
- Vetter, W., Darwisch, V., Lehnert, K., 2020. Erucic acid in Brassicaceae and salmon – An evaluation of the new proposed limits of erucic acid in food. *NFS Journal* 19, 9-15. <https://doi.org/10.1016/j.nfs.2020.03.002>.
- Wang, E., Ma, X., Tang, S., Yan, R., Wang, Y., Riley, W.W., Reaney, M.J.T., 2014. Synthesis and oxidative stability of trimethylolpropane fatty acid triester as a biolubricant base oil from waste cooking oil. *Biomass and Bioenergy* 66, 371-378. <http://dx.doi.org/10.1016/j.biombioe.2014.03.022>.
- Zheng, T., Wu, Z., Xie, Q., Lu, M., Xia, F., Wang, G., Nie, Y., Ji, J., 2018. Biolubricant Production of 2-Ethylhexyl Palmitate by Transesterification Over Unsupported

Potassium Carbonate. *Journal of American Oil Chemical Society* 95, 79-88.
<https://doi.org/10.1002/aocs.12023>.

FIGURES

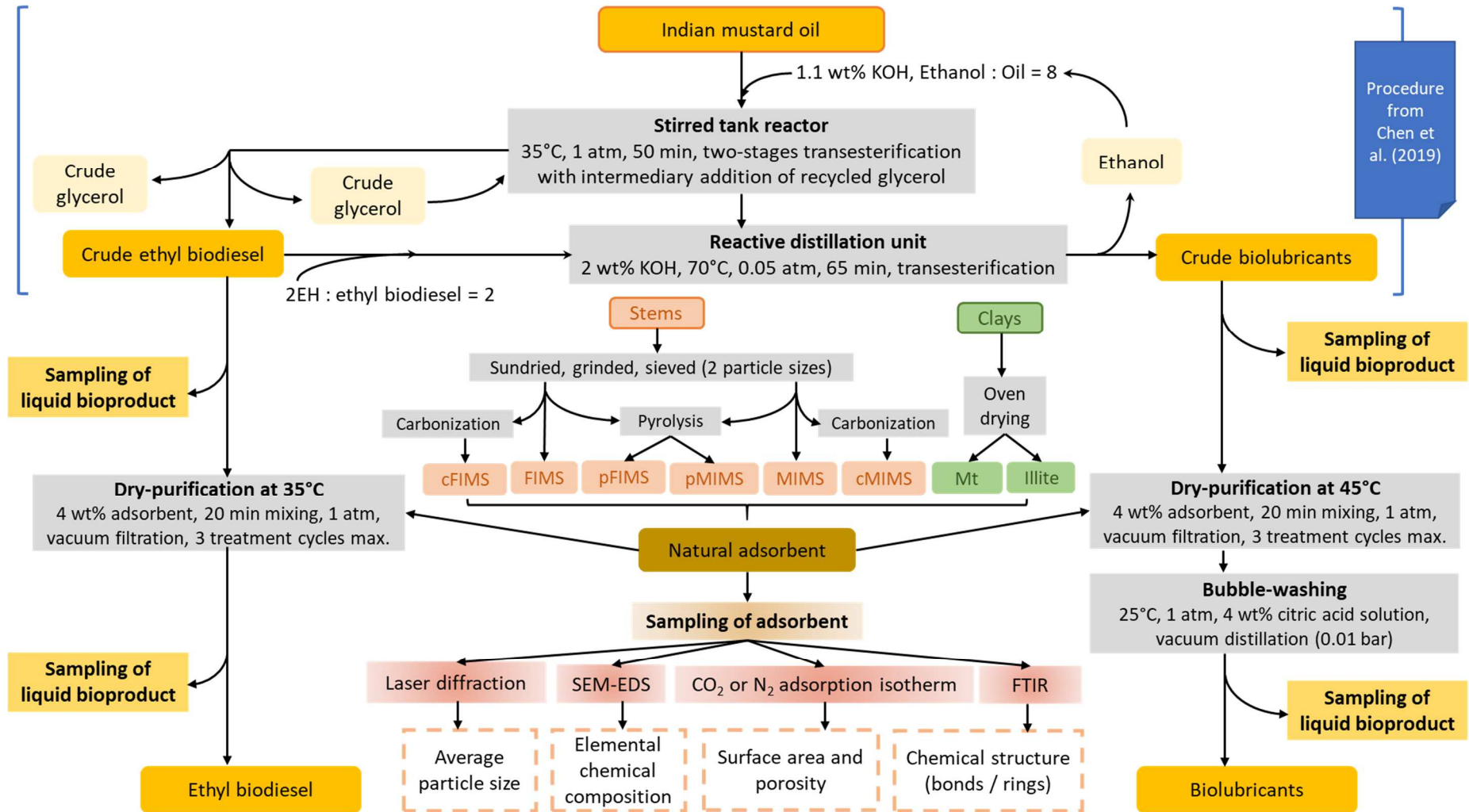


Figure 1. Methodology, experimental technics and properties selected for characterizing the bioproduct samples and optimizing the purification procedure.

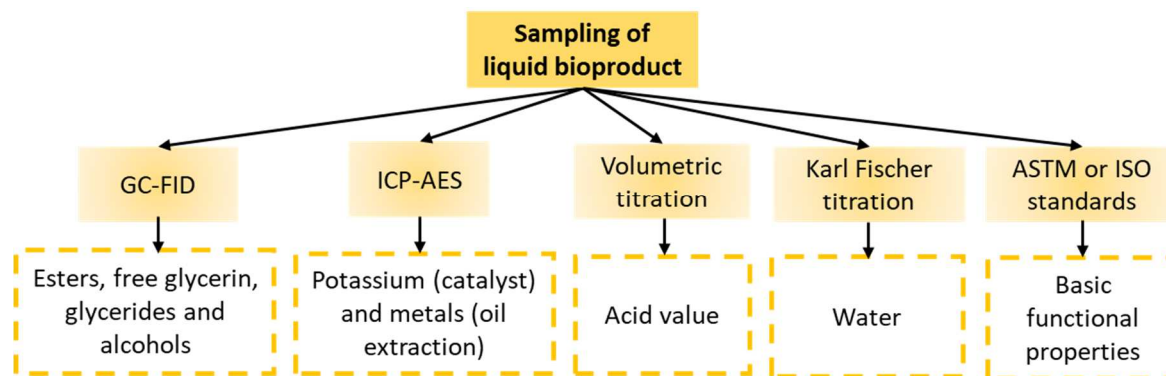
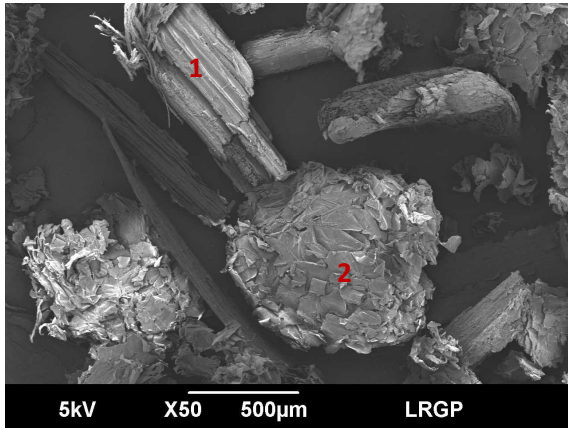
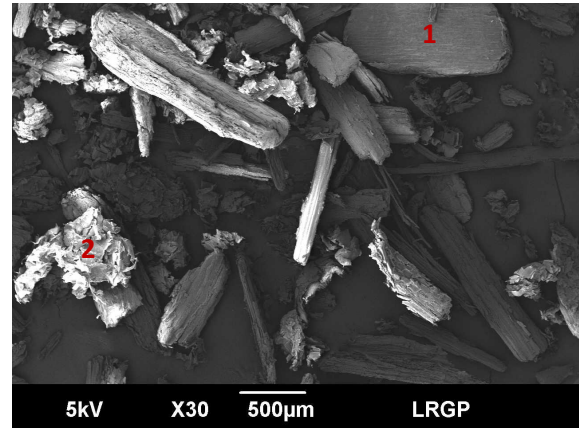


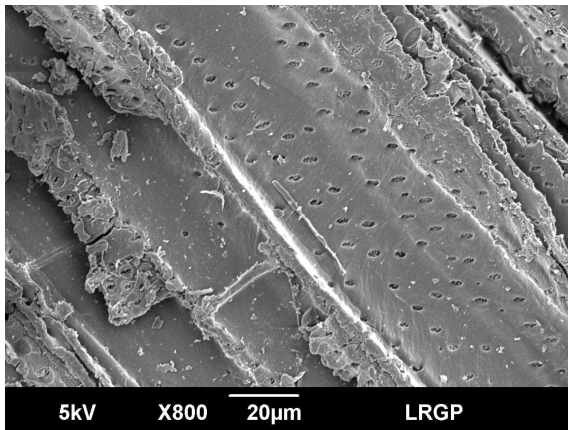
Figure 1. Continued.



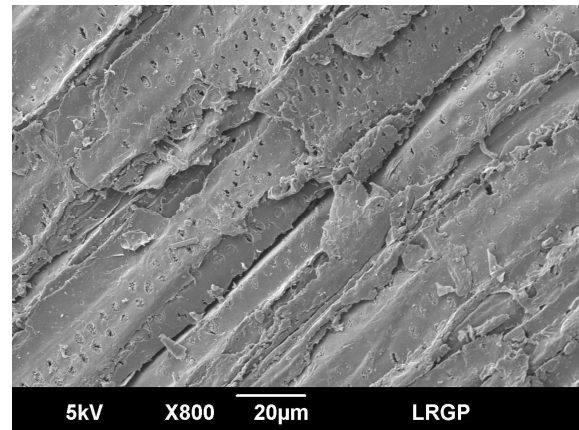
(a) FIMS; elements (wt%) related to point 1 (bark) and point 2 (core): see respectively **(a₁)** and **(a₂)** below.



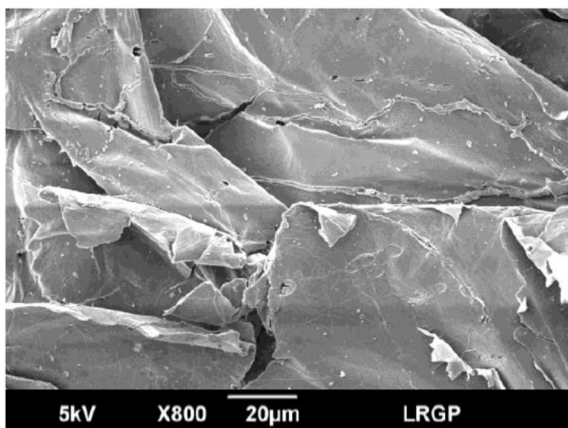
(b) MIMS; elements (point 1, bark; point 2, core; both $\times 800$) (wt%): C (46.8; 41.0), O (38.5; 40.7), Na (1.4; 0.8), Mg (0.7; 0.2), Al (0.4; 0.2), Si (0.7; 0.0), S (0.5; 0.4), Cl (0.5; 3.4), K (1.6; 3.0), Ca (3.7; 2.5) [coating Pd (1.0), Au (4.2)]; *Ca/K* (2.3; 0.8), *C/O* (1.2; 1.0).



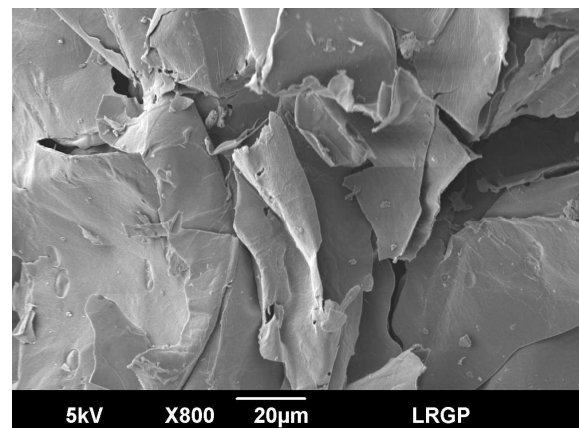
(a₁) FIMS bark; elements (wt%): C (49.0), O (39.6), Na (0.6), Mg (0.3), Al (0.2), Si (0.1), S (1.2), Cl (0.7), K (1.7), Ca (2.2) [coating Pd (1.1), Au (4.9)]; *Ca/K* (1.3), *C/O* (1.2).



(c₁) pFIMS bark; elements (wt%): C (71.4), O (13.4), Na (1.4), Mg (0.5), Al (0.3), Si (0.2), P (0.3), S (0.7), Cl (0.2), K (0.7), Ca (1.0) [coating Pd (1.6), Au (8.6)]; *Ca/K* (1.4), *C/O* (5.3).



(a₂) FIMS core; elements (wt%): C (39.9), O (45.0), Na (0.7), Mg (0.6), Al (0.2), Si (0.2), S (0.9), Cl (0.9), K (2.6), Ca (2.9) [coating Pd (1.1), Au (4.8)]; *Ca/K* (1.1), *C/O* (0.9).



(c₂) pFIMS core; elements (wt%): C (67.0), O (16.7), Na (1.1), Mg (0.6), Al (0.2), Si (0.2), P (0.1), S (0.4), Cl (0.2), K (2.7), Ca (2.6) [coating Pd (1.5), Au (7.2)]; *Ca/K* (1.0), *C/O* (4.0).

Figure 2. SEM/EDS analyses of the organic adsorbents prepared in this work (secondary electrons with palladium-gold coating).

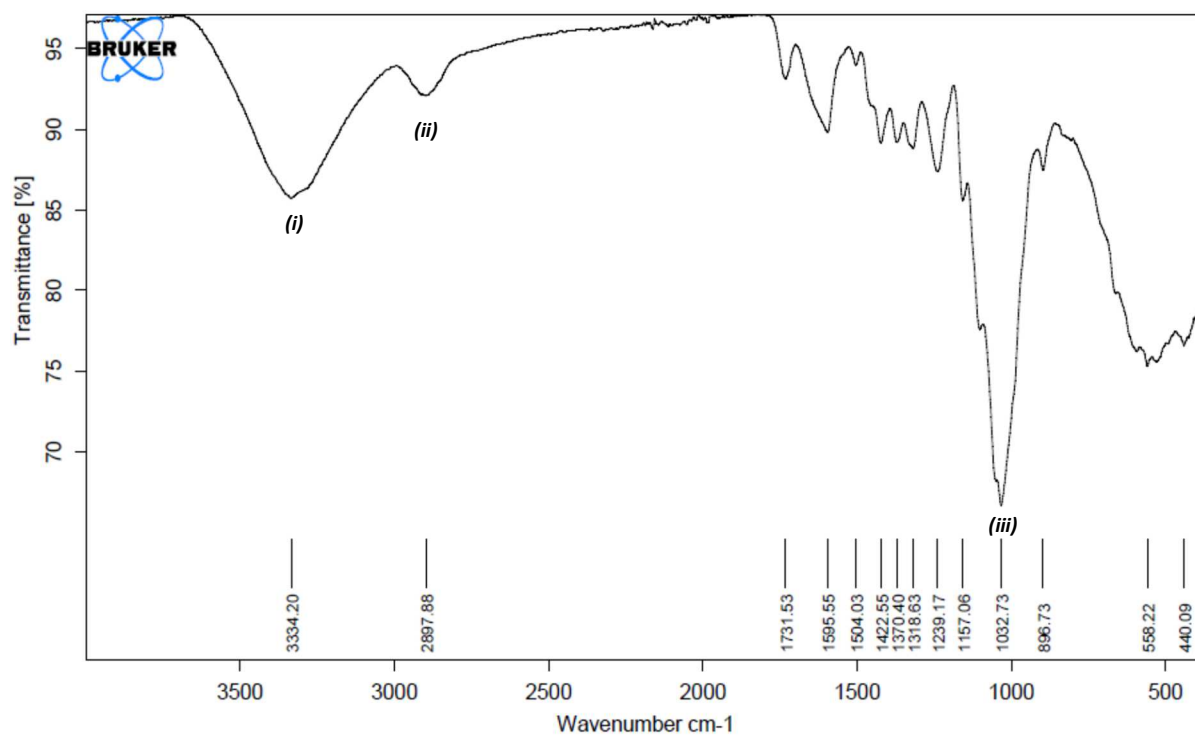


Figure 3. FTIR spectra of FIMS (Mazivila et al., 2015; Feng et al., 2018). (i) free hydroxyl O-H stretching at the range of 3500 to 3300 cm⁻¹, (ii) alkyl C-H stretching at 2898 cm⁻¹, (iii) etheric C-O stretching at 1033 cm⁻¹.

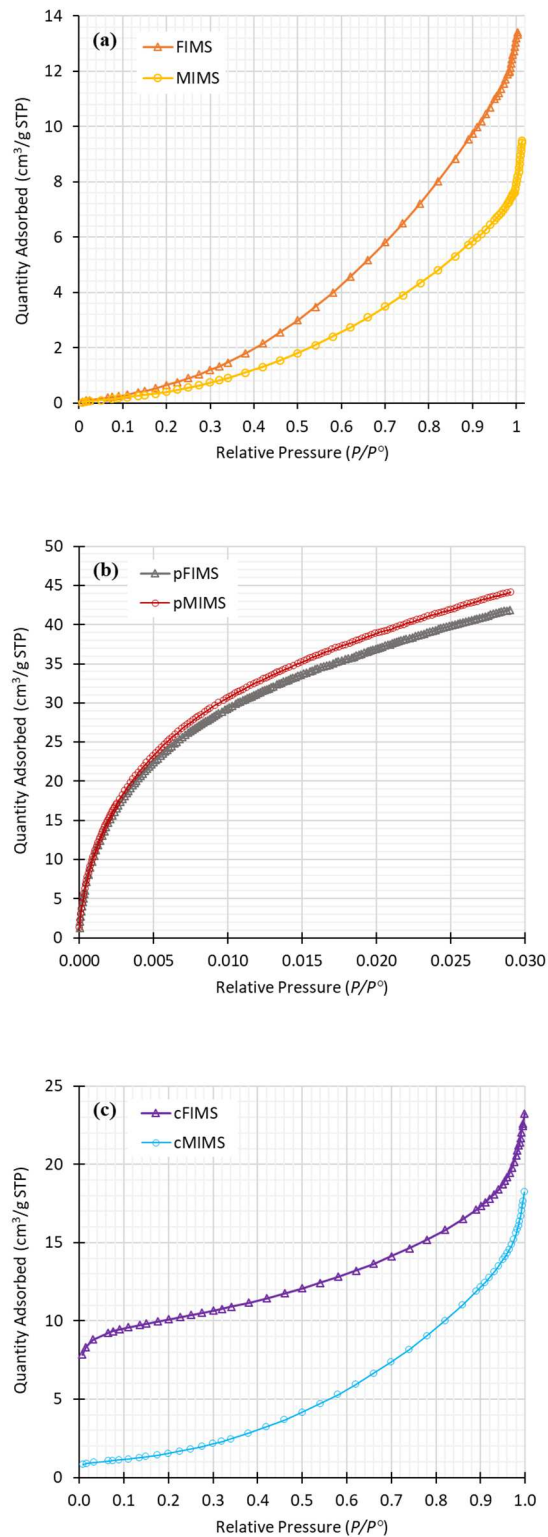


Figure 4. N₂ or CO₂ adsorption isotherms of the prepared organic adsorbents; **(a)** FIMS and MIMS (N₂, 77 K); **(b)** pFIMS and pMIMS (CO₂, 273 K); **(c)** cFIMS (CO₂, 273 K) and cMIMS (N₂, 77 K). P^o is the saturation pressure of the pure adsorptive (N₂ or CO₂) at the operational temperature (77 K or 273 K).

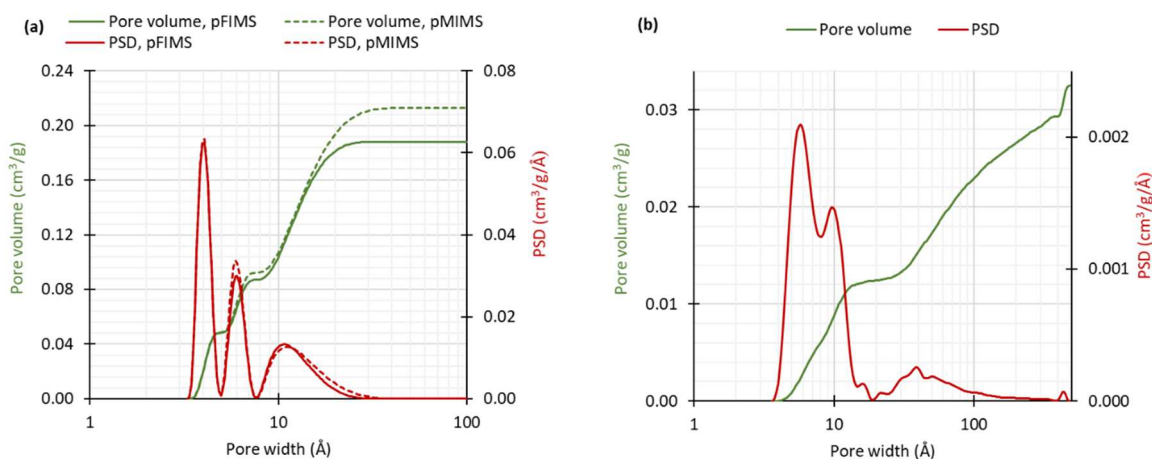


Figure 5. Pore size distribution and cumulative pore volume versus pore width for pyrolyzed and carbonized Indian mustard stems; **(a)** pFIMS and pMIMS; **(b)** cFIMS.

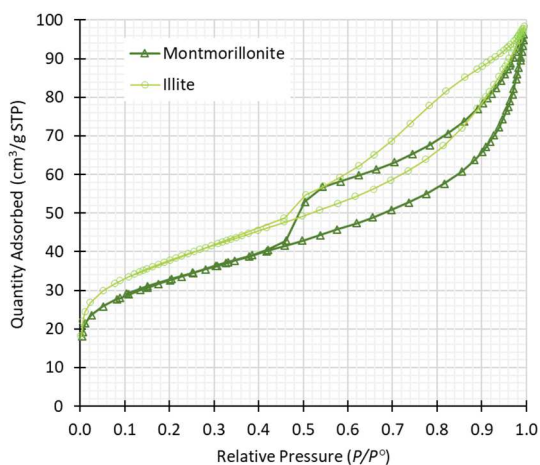


Figure 6. N₂ adsorption-desorption isotherms at 77 K for the selected mineral adsorbents; **(a)** Montmorillonite, **(b)** Illite). P° is the saturation pressure of the pure adsorptive (N₂) at the operational temperature (77 K).

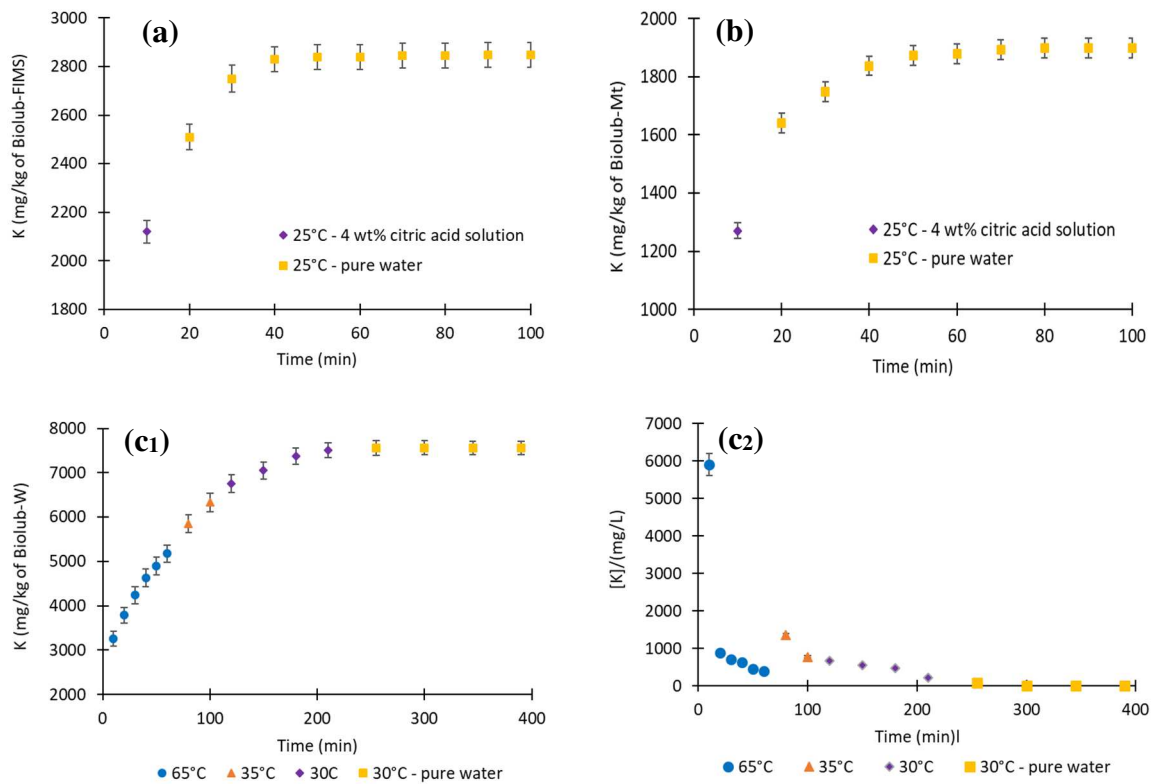


Figure 7. Further wet-purification for the biolubricant samples obtained after dry-treatment **(a)** Biolub-FIMS and **(b)** Biolub-Mt; **(c)** Comparison with the biolubricant sample Biolub-W purified exclusively by bubble-washing; **(c1)** [K] (mg/L) or **(c2)** cumulative K content (mg/kg departure Biolub) in the aqueous phase recovered during the successive bubble-washing cycles. Estimated averages and standard deviations of the experimental data are presented in the figure as error bars.

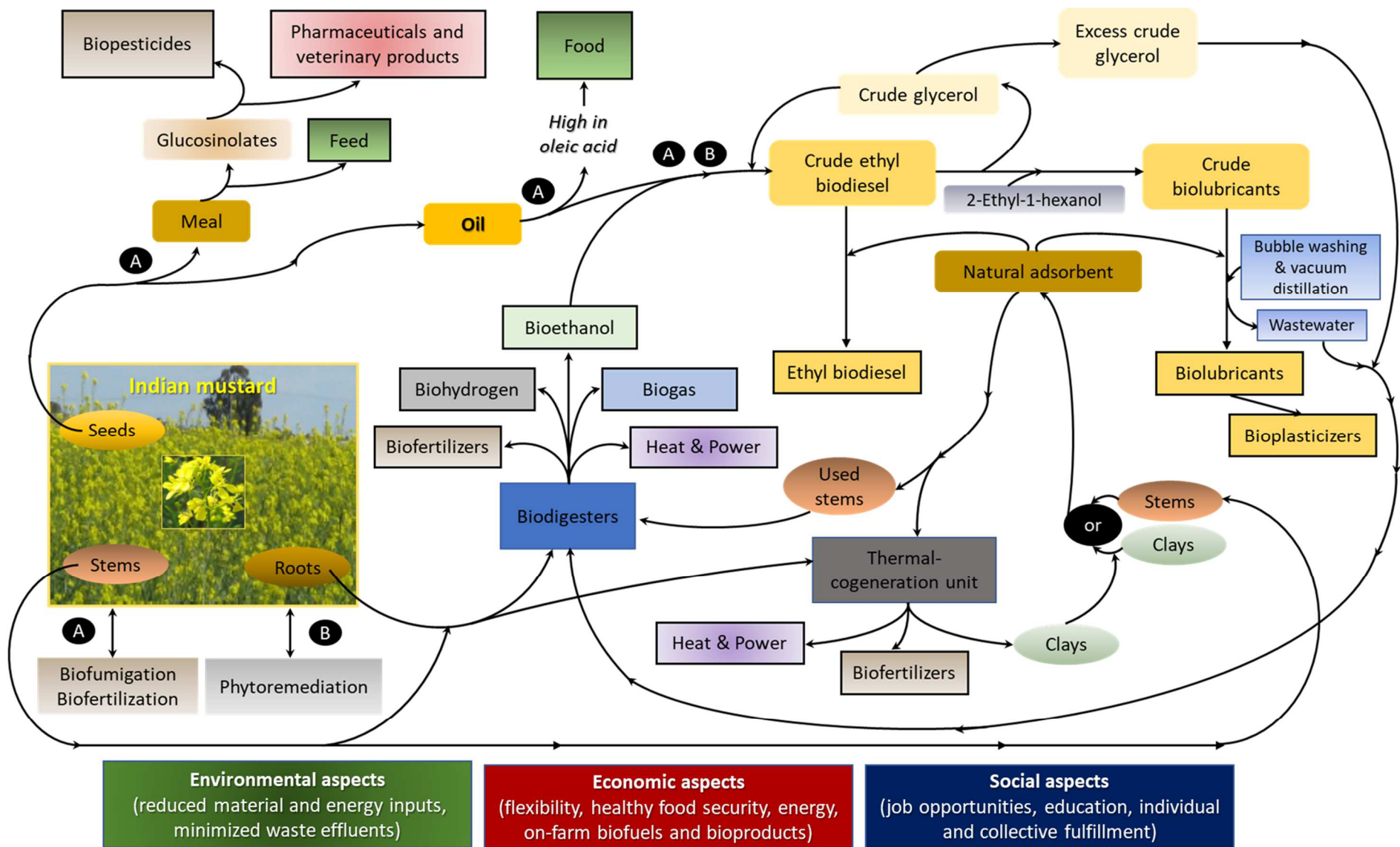


Figure 8. Main keyword network of the biorefinery focused on Indian mustard.

TABLES

Table 1. Analysis equipment and operating conditions selected for the adsorbent characterization.

Objective	Experimental technique	Equipment	Operating conditions
Average particle size (Sauter mean diameter) D[3,2]	Laser diffraction	Malvern Master sizer 2000 (UK)	Size range: 0.02 to 2000 μm
Morphology	SEM	JEOL microscope; model JSM-6490 LV (Japan)	Nitièma-Yefanova et al. (2015)
Elemental chemical composition	SEM-EDS	JEOL microscope; model JSM-6490 LV (Japan) + SAMX-IDFIX system (microanalysis) (France)	Nitièma-Yefanova et al. (2015)
Surface area and porosity	CO ₂ (273 K) or N ₂ (77 K) adsorption isotherm + 2D-NLDFT, Dubinin-Astakhov or BET method	Micromeritics Tristar II Plus (USA) Micromeritics 3Flex (USA)	Nitièma-Yefanova et al. (2015)
Chemical structure (bonds/rings)	FTIR	Bruker Alpha-P spectrophotometer, equipped with an Attenuated Total Reflectance (ATR) crystal accessory (Switzerland)	For each spectrum: 128 scans applied at a resolution of 4 cm^{-1} with the wavenumber ranging from 4000 to 375 cm^{-1}

Table 2. Physical properties of the organic adsorbents prepared in this work.

Physical characteristic	Organic adsorbent					
	FIMS	MIMS	pFIMS	pMIMS	cFIMS	cMIMS
Average particle size D[3,2] (μm) ^a	284.376	-	254.561	498.911	11.276	4.953
Smallest particle diameter (μm) ^a	30.200	-	10.000	11.482	0.479	0.240
Specific surface area (m^2/g) ^b	< 6	< 6	526	561	37.8	6.46
Pore volume (cm^3/g) ^b	-	-	0.19	0.21	0.032	-
Mean pore width (Å) ^b	-	-	15.9	15.9	-	-

^a Sauter mean diameter measured by laser diffraction; MIMS particles were too large to measure these properties. ^b Determined by CO₂ (273 K) or N₂ (77 K) adsorption isotherms with 2D-NLDFT, Dubinin--Astakhov or BET method. ^{a,b} Equipment details in **Table 1** of this work.

Table 3. Average chemical composition and physical properties of the natural clays selected as mineral adsorbents (EMSPAC, 2019).

(a) Average chemical composition (wt%)

Species	Montmorillonite (Mt)	Illite
SiO ₂	55.47	52.12
Al ₂ O ₃	18.64	16.65
MgO	4.01	2.16
Fe ₂ O ₃	6.35	5.65
Na ₂ O	1.10	0.06
CaO	1.93	2.41
K ₂ O	3.66	2.70
MnO	0.15	0.00
TiO ₂	0.00	0.64

(b) Physical properties

Property	Montmorillonite (Mt)	Illite
Average particle size D [3,2] (μm) ^a	10.472	5.871
Smallest particle diameter (μm) ^a	0.479	0.316
Specific surface area (m ² /g) ^b	117	135
Pore volume (cm ³ /g) ^b	0.055	0.064
Mean pore width (Å) ^b	18.8	19.1
Moisture level (%) ^c	2 to 3	2 to 3
Appearance ^c	Dark green fine powder	Light green fine powder
PH ^c	Neutral	Neutral
Density (g/cm ³) ^c	1	0.95
Solubility ^c	None in water or organic solvents	None in water or organic solvents

^a Sauter mean diameter by measured by laser diffraction. ^b Determined from N₂ adsorption-desorption isotherms at 77 K by using Dubinin-Astakhov method. ^{a,b} Equipment details in **Table 1** of this work.

Table 4. Characterization of the produced biofuel before and after dry-purification over different adsorbents ^a

Adsorbent - Treatment cycle	Molecular components ^b						Chemical elements ^d			
	Esters (wt%) (η_c %)	Free glycerin (wt%) (η_c %)	MGs (wt%) (η_c %)	DGs (wt%) (η_c %)	TGs (wt%) (η_c %)	Total glycerin (wt%) (η_c %)	Water (mg/kg) (η_c %)	Acid number (mg KOH/g) (η_c %)	Ca (mg/kg) (η_c %)	K (mg/kg) (η_c %)
Crude IMSOEEs of departure	88.5	0.0600	2.58	0.75	0.27	0.86	343	0.43	< 0.001	104.870
FIMS-1	95.0 (7)	0.0413 (-31)	2.50 (-3)	0.56 (-25)	0.25 (-7)	0.79 (-9)	647 (89)	0.40 (-7)	1.452 (NA)	< 0.031 (-100)
FIMS-2	95.3 (8)	0.0154 (-74)	2.48 (-4)	0.54 (-28)	0.23 (-15)	0.75 (-13)	560 (63)	0.36 (-16)	0.378 (NA)	< 0.031 (-100)
FIMS-3	95.8 (8)	0.0098 (-84)	2.46 (-5)	0.53 (-29)	0.22 (-19)	0.74 (-14)	412 (20)	0.34 (-21)	< 0.001 (-)	< 0.031 (-100)
MIMS-1	93.2 (5)	0.0477 (-21)	2.55 (-1)	0.56 (-25)	0.25 (-7)	0.81 (-6)	647 (89)	0.42 (-2)	16.385 (NA)	43.167 (-59)
MIMS-2	94.0 (6)	0.0187 (-69)	2.49 (-3)	0.53 (-29)	0.24 (-11)	0.76 (-12)	625 (82)	0.40 (-7)	11.647 (NA)	< 0.031 (-100)
MIMS-3	94.6 (7)	0.0153 (-75)	2.48 (-4)	0.53 (-29)	0.22 (-19)	0.75 (-13)	463 (35)	0.38 (-12)	5.086 (NA)	< 0.031 (-100)
pFIMS-1	96.0 (8)	0.0377 (-37)	2.55 (-1)	0.55 (-27)	0.24 (-11)	0.79 (-8)	683 (99)	0.43 (0)	< 0.001 (-)	24.571 (-77)
pFIMS-2	96.1 (9)	0.0138 (-77)	2.53 (-2)	0.54 (-28)	0.23 (-15)	0.76 (-11)	574 (67)	0.42 (-1)	< 0.001 (-)	22.104 (-79)
pFIMS-3	96.4 (9)	0.0093 (-85)	2.51 (-3)	0.52 (-31)	0.21 (-22)	0.75 (-13)	493 (44)	0.40 (-7)	< 0.001 (-)	12.559 (-88)
pMIMS-1	93.6 (6)	0.0391 (-35)	2.54 (-2)	0.57 (-24)	0.24 (-11)	0.79 (-8)	646 (88)	0.43 (0)	< 0.001 (-)	43.256 (-59)
pMIMS-2	94.3 (7)	0.0167 (-72)	2.52 (-2)	0.54 (-28)	0.23 (-15)	0.76 (-11)	579 (69)	0.43 (0)	< 0.001 (-)	24.523 (-77)
pMIMS-3	95.4 (8)	0.0095 (-84)	2.51 (-3)	0.54 (-28)	0.22 (-19)	0.75 (-13)	441 (29)	0.42 (-2)	< 0.001 (-)	18.339 (-83)
cFIMS-1	93.2 (5)	0.0407 (-32)	2.49 (-3)	0.52 (-31)	0.21 (-22)	0.77 (-10)	598 (74)	0.36 (-16)	< 0.001 (-)	15.190 (-86)
cMIMS-1	95.0 (7)	0.0454 (-24)	2.53 (-2)	0.52 (-31)	0.21 (-22)	0.79 (-8)	436 (27)	0.40 (-7)	< 0.001 (-)	7.153 (-93)
Mt-1	94.2 (6)	0.0213 (-65)	2.32 (-10)	0.55 (-27)	0.26 (-4)	0.72 (-16)	366 (7)	0.29 (-32)	< 0.001 (-)	< 0.031 (-100)
Mt-2	95.1 (7)	0.0128 (-79)	2.04 (-21)	0.53 (-29)	0.25 (-7)	0.64 (-26)	364 (6)	0.17 (-60)	< 0.001 (-)	< 0.031 (-100)
Mt-3	96.3 (9)	0.0090 (-85)	1.92 (-26)	0.52 (-31)	0.25 (-7)	0.60 (-30)	320 (-7)	0.11 (-74)	< 0.001 (-)	< 0.031 (-100)
Illite-1	93.8 (6)	0.0279 (-54)	2.48 (-4)	0.53 (-29)	0.25 (-7)	0.76 (-11)	370 (8)	0.33 (-23)	< 0.001 (-)	< 0.031 (-100)
Illite-2	94.9 (7)	0.0117 (-81)	2.46 (-5)	0.52 (-31)	0.24 (-11)	0.74 (-14)	368 (7)	0.21 (-51)	< 0.001 (-)	< 0.031 (-100)
Illite-3	95.8 (8)	0.0062 (-90)	2.43 (-6)	0.51 (-32)	0.23 (-15)	0.72 (-16)	335 (-2)	0.15 (-65)	< 0.001 (-)	< 0.031 (-100)
Specifications of EN-14214 ^e	96.5	0.0200	0.80	0.20	0.20	0.25	500	0.50	5.000 ^e	5.000 ^f

^a Method efficiency given in brackets is assessed as a function of removal percentage of each component (η_c) calculated by $\eta_c = 100 \times (x_f - x_0) / x_0$, where x_0 and x_f are the contents of each component before and after treatment. ^b Standard deviations (wt%): 0.08 on esters, 0.003 on free glycerin, 0.05 on MGs, DGs, and TGs; standard deviations for the others: 20 mg/kg on water, 0.02 mg KOH/g for the acid number. ^c All indications are maximum limits, except for the ester content giving the minimum value. ^d Detection limits (mg/kg) of the analytical method used (ICP-AES): 0.001 for Ca and Mg; 0.003 for Fe; 0.031 for K; 0.073 for Na; 0.006 for P; 0.038 for S; Maximum standard deviation (mg/kg): 0.001 for Ca, Mg, Fe, and P; 0.05 for Na; 0.01 for K and S; regarding contaminant content below or equal to the observed ICP-AES detection limit, this latter value was used to evaluate the treatment efficiency. It should be mentioned that some other metals have not been detected (Ag, Al, As, B, Ba, Cd, Co, Cr, Cu, Fe, Hg, Li, Mg, Mn, Mo, Na, Ni, P, Pb, S, Sb, Sr, Ti, V, and Zn). *NA* means “Non-acceptable”. ^e For (Ca + Mg). ^f For (Na + K).

Table 5. Some functional properties and ester composition of the biofuel and biolubricant obtained according to the various purification methods tested ^a

(a) Functional properties

Property	Biofuel-FIMS-3	Biofuel-Mt-3	Biofuel-Illite-3	Biodiesel specifications [min ; max]	Biolub-FIMS-W&D	Biolub-Mt-W&D	Biolub-W&D	Biolub-Ref. (Valtris, 2019) ^b	Standard deviations ^c
Acid value (mg KOH/g)	0.34	0.11	0.15	[- ; 0.50]	8.6	0.45	12.2	0.5	± 0.02
Color (Gardner)	10.4	7.8	10.4	[- ; -]	7.2	5.8	4.7	1.0	± 0.2
Density (kg/m ³)	882 ^(15°C)	881 ^(15°C)	881 ^(15°C)	[860 ^(15°C) ; 900 ^(15°C)]	875 ^(20°C)	873 ^(20°C)	875 ^(20°C)	870 ^(20°C)	± 3·10 ⁻⁵
Viscosity (mm ² /s) at 40°C	5.0	4.9	4.9	[3.5 ; 5.0]	8.7	8.0	8.6	9.0	± 0.1
at 100°C				[- ; -]	2.8	2.7	2.8	3.0	± 0.1
Flash point (°C)	425	425	425	[101 ; -]	-	-	-	200	± 12
Cloud point (°C)	-5	-5	-5	[-12 ; -3]	-	-	-	-	± 1
Pour point (°C)	-9	-9	-8	[-16 ; -5]	-	-	-	-69	± 2
Cold filter plugging point (°C)	-11	-11	-11	[- ; -]	-	-	-	-	-
Higher heating value (MJ/kg) ^d	41.50	41.50	41.50	[- ; -]					
Oxidation stability at 110°C (hrs) ^d	6.40	6.39	6.44	[6 ; -]					

(b) Percent mass composition of the identified esters (IMSOEEs for the biofuel samples; IMSO2EHES for the biolubricant samples)

Liquid bioproduct	C16:0	C18:0	C18:1 (oleate)	C18:1 (cis-vaccenate)	C18:2	C18:3	C20:1	C22:1
Biofuel-FIMS-3	3.41	2.14	33.82	2.56	27.03	14.57	6.02	6.26
Biofuel-Mt-3	3.49	2.25	34.96	2.71	27.76	14.72	4.55	5.85
Biofuel-Illite-3	3.47	2.24	34.84	2.63	27.63	14.65	4.52	5.82
Biolub-FIMS-W&D ^e	3.49 (0.05)	2.20 (0.03)	33.74 (0.49)	2.59 (0.04)	26.43 (0.40)	13.60 (0.20)	5.39 (0.07)	5.42 (0.08)
Biolub-Mt-W&D ^e	3.55 (0.18)	2.25 (0.26)	34.18 (1.92)	2.63 (0.15)	26.19 (1.46)	13.23 (0.73)	4.64 (0.25)	5.50 (0.31)
Biolub-W&D ^e	3.35 (0.19)	2.11 (0.19)	32.17 (2.01)	2.49 (0.15)	24.77 (1.57)	12.57 (0.79)	5.63 (0.27)	5.25 (0.33)

^a Please, refer to [Chen et al. \(2019\)](#) in Appendix A for details regarding the methods leading to the given property values. All biofuel samples were obtained after 3 cycles of dry-purification. All biolubricant samples were obtained after a single dry-purification followed by bubble-washing (W) until reaching a constant K content in the washing solution, and then vacuum distillation (D). These samples are referenced as following: liquid bioproduct–adsorbent–number of treatment cycle (recalled only for the biolubricant samples)–further treatment when existing. ^b This biolubricant was produced with the same alcohol as the one selected in this work (2EH) but with rapeseed oil. ^c These standard deviations are common to determination of both biofuel and biolubricant specific functional properties. ^d Properties estimated from [Hong et al. \(2014\)](#) method. ^e In brackets, are given the percent mass fractions of the remaining IMSOEEs.

Table 6. Characterization of the produced biolubricant according to the purification methods ^a

Species	Crude Biolub	Biolub-FIMS	Biolub-FIMS-W&D	Biolub-Mt	Biolub-Mt-W&D	Biolub-W&D
K (mg/kg)	7562	2849 (-62)	0.91 (-100)	1899 (-75)	0.35 (-100)	0.29 (-100)
2EH (wt%)	20.49	20.50 (0)	0.18 (-99)	20.32 (-1)	0.85 (-96)	Not detected (-100)
Ethanol (wt%)	0.02	0.02 (0)	Not detected (-100)	0.01 (-50)	Not detected (-100)	Not detected (-100)
IMSOEEs (wt%)	4.25	1.56 (-63)	1.34 (-68)	4.17 (-2)	5.26 (24)	5.50 (29)
IMSO2EHes (wt%)	69.71	73.43 (5)	92.88 (33)	72.37 (4)	92.18 (32)	88.34 (27)

^a Method efficiency given in brackets is assessed as a function of removal percentage of each component (η_c) calculated by $\eta_c = 100 \times (x_f - x_0) / x_0$, where x_0 and x_f are the contents of each component before and after treatment. All biolubricant (Biolub) samples were obtained after a single dry-purification (FIMS or Mt) followed by bubble-washing (W) until reaching a constant K content in the washing solution, and then vacuum distillation (D). ^b Standard deviations for esters and alcohols quantified by GC-FID: 0.04 wt%; for K quantification by ICP-AES, detection limit and maximum standard deviation: 0.031 and 0.01 mg/kg, respectively (Chen et al., 2019; Appendix A).

Table 7. Revenue projection for Indian mustard oil over 5 years (2021-2026) from planting to processing plant (**Rapp and Kemp, 2020**).

Parameters	Multiplying factor	Factor units	Factor source	Year					
				2021	2022	2023	2024	2025	2026
•Planting information									
Total area sown (ha)				5	1 000	1 600	2 000	3 000	4 000
Total amount of seed planted (kg)	2.0	(kg / ha)	Sowing rate recommended by NSW government DPI	10	2000	3200	4000	6000	8000
Total yield of seeds (ton/ha)	1.5	(ton / ha)	From personal experience	7.5	1500	2400	3000	4500	6000
Seeds for planting (ton)				2	3.2	4	6	8	10
Surplus of seeds (ton)				5.5	1497	2396	2994	4492	5990
Seed value Ex-farm to the processing plant (AUD) - α	750	(AUD / ton)	NSW government DPI	4 125	1 122 600	1 797 000	2 245 500	3 369 000	4 492 500
•Indian mustard oil information									
Mustard oil obtained (Litre)	300	Litre of mustard oil / ton of seeds	Rapp (2018)	1 650	449 040	718 800	898 200	1 347 600	1 797 000
Premium mustard oil value (AUD) - β	5	AUD / Litre of mustard oil	Yandilla mustard oil enterprise (Australia)	8 250	2 245 200	3 594 000	4 491 000	6 738 000	8 985 000
Mustard oil for biodiesel or biolubricant value (AUD)	0.65	AUD / Litre of mustard oil	BioCube (Canada)	1 073	291 876	467 220	583 830	875 940	1 168 050
Biodiesel (B100, B20, B5) cost at the bowser (AUD)	1.3	AUD / Litre of biodiesel at the bowser	Base price in Australia	2 145	583 752	934 440	1 167 660	1 751 880	2 336 100

Table 7. Continued.

Parameters	Multiplying factor	Factor units	Factor source	Year					
				2021	2022	2023	2024	2025	2026
•Biofumigation related information (cereal: wheat, barley, rye, oats and triticale ^b)									
Methyl bromide costs (AUD)	350	AUD / ha	Retail price in Australia	1 750	350 000	560 000	700 000	1 050 000	1 400 000
Cereal yield base amount (avg., ton)	4.5	ton / ha	Personal experience	23	4 500	7 200	9 000	13 500	18 000
Increase in cereal yield for year 1 (ton)	20	% increase in ton / ha	Rapp (2018)	27	5400	8640	10800	16200	21600
Increase in cereal yield for year 2 (ton)	20	% increase in ton / ha	Rapp (2018)	32	6480	10368	12960	19440	25920
Return of cereal at the market price (AUD)	400	AUD / ton	Personal experience	9 000	1 800 000	2 880 000	3 600 000	5 400 000	7 200 000
Income return from the increase in cereal yield for year 1 (AUD)	400	AUD / ton	Personal experience; assuming no price rise for years 1 and 2	10 800	2 160 000	3 456 000	4 320 000	6 480 000	8 640 000
Income return from the increase in cereal yield for year 2 (AUD)	400	AUD / ton	Personal experience; assuming no price rise for years 1 and 2	12 960	2 340 000	4 147 200	5 184 000	7 776 000	10 368 000
Total value (soil biofumigation savings by avoiding methyl bromide use & cereal yield improvement) (AUD) - (γ)				34 510	6 650 000	11 043 200	13 804 000	20 706 000	27 608 000
Total revenue per year (AUD) - ($\alpha + \beta + \gamma$)				46 885	10 017 800	16 434 200	20 540 500	30 813 000	41 085 500
Total revenue after 5 years (AUD)									118 937 885

^a Estimations made from study carried out by **Rapp (2018)**; area(ha): 5; period (year): 2013 to 2015; amount of seeds planted (kg/ha): 2; ^b Triticale was developed by human intervention from crosses between wheat (genus Triticum) and rye (genus Secale).

Table 8. Main characteristics of methods used to produce biofuels similar to petrodiesel from various biomass resources (Coniglio et al., 2013; Coniglio et al., 2014; Nitièma-Yefanova et al., 2016; Kargbo et al., 2021).

Feedstock	Conversion method	Advantages	Drawbacks
Lignocellulosic biomass	1- Thermochemical routes leading to drop-in fuels, i.e. liquid hydrocarbons with functionally equivalent to fossil fuels and fully compatible with existing infrastructures: 1.1-Biomass-to-liquid (BTL) and 1.2-Fast pyrolysis		
	1.1-Biomass-to-Liquid (BTL): gasification (under air, oxygen and steam) → syngas purification → Fischer- Tropsch Synthesis (FTS), leading to FTS-biofuel (diesel, and also gasoline and jet fuel)	<ul style="list-style-type: none"> •Flexibility towards feedstock acceptance; •Production with high yields of drop-in fuels; •Fuels with improved combustion and emission performance (high cetane number and low NOx formation); •Integrated polygeneration system (heat and power) 	<ul style="list-style-type: none"> •For FTS: $H_2/CO \geq 2$, which is highly inflammable; •High temperature (200°C – 350°C); • Biomass pretreatment (size reduction and drying), syngas clean-up (to prevent catalyst deactivation) and FTS-biofuel fractionation consuming up to 15% feedstock energy and increasing cost production; •Technology well established from coal, but incorporation of biomass feedstock for syngas production and subsequent upgrading in drop-in fuels still in early commercialization stage
	1.2-Fast pyrolysis (under nitrogen) to produce bio-oil (main product), gas and char; → For bio-oil: series of catalytic upgrading hydrotreatment (hydrodeoxygenation, then hydrocracking)	<ul style="list-style-type: none"> •Low reaction time (2 s); •Wide range of feedstock (including waste plastics); •Commercialized for bio-oil production with heat and power generation 	<ul style="list-style-type: none"> •High temperature (450°C-550°C); •High pressure (10 MPa); •Moisture < 10 wt%; •Catalytic deactivation during upgrading due to water and oxygenated compounds; •Upgrading process still at the prototype stage
	2. Biochemical routes in the presence (aerobic fermentation) or absence (anaerobic fermentation) of air to produce alcohols (ethanol, butanol); → Alcohols recovery and purification → Upgrading by hydrotreatment to produce drop-in fuels	<ul style="list-style-type: none"> •Mild operating conditions (37°C - 42°C; 0.1 MPa; PH = 4.5) 	<ul style="list-style-type: none"> •Preliminary steps to fermentation: pretreatment (size reduction, thermochemical) followed by enzymatic hydrolysis; •Low yield (40 to 50 wt%); •High energy input for product extraction; •High cost of enzyme

Table 8. Continued.

Feedstock	Conversion method	Advantages	Drawbacks
Algae and other wet feedstock such as sludge, manure...	Hydrothermal liquefaction (HTL) to produce bio-crude oil requiring then upgrading by a series of catalytic treatment to produce drop-in fuels	<ul style="list-style-type: none"> •Water up to 80 wt%; •Water acts both as a reactant and a catalyst; •Bio-crude oil requiring less extensive upgrading than pyrolysis bio-oil; •Suitable for biodiesel production (but hydrocracking required to obtain jet fuel and/or gasoline) 	<ul style="list-style-type: none"> •High temperature (250°C - 550°C); •High pressure (5 MPa - 25 MPa); •High separation costs between bio-oil and aqueous components; •Disposal of wastewater; •High capital and operational costs (corrosion prevention, high pressure, wastewater treatment and recycling); •Upgrading process still at the lab tests
Triglycerides (from non-edible oils, waste cooking oil)	<p>1- Transesterification: methanolysis or ethanolysis of triglycerides to produce (in addition of glycerin as by-product) fatty acid methyl- or ethyl esters, respectively known as commercial “(methyl) biodiesel” (produced at industrial scale) and “ethyl biodiesel”</p> <p>1.1-Homogeneous catalysis</p> <p>1.2-Heterogeneous catalysis</p>	<p><i>Alkaline:</i> •High catalytic efficiency; •High yield (96 wt%); •Quite short reaction time (60 min); •Quite low temperature (65°C); •Low pressure (0.1 MPa); •Low alcohol to oil molar ratio (6:1); •Cheap</p> <p><i>Acid:</i> •Efficient for high FFA oils (> 3 wt%)</p> <p><i>Alkaline:</i> •Higher catalytic activity than heterogeneous acid catalyst</p> <p><i>Acid:</i> •Catalyzes both esterification and transesterification of triglycerides</p> <p><i>Alkaline and acid:</i> catalyst easily recovered and can be reused</p>	<p><i>Alkaline:</i> •Very sensitive to the presence of FFAs and water</p> <p><i>Acid:</i> •Low catalytic activity inducing long reaction time (120 min); •Highly sensitive to the presence of water;</p> <p>•Corrosive</p> <p><i>Alkaline and acid:</i> •Catalyst not recovered and generation of wastewater</p> <p><i>Alkaline and acid:</i> •High catalyst cost; •Moderate to high reaction temperature (70°C – 120°C); •Water tolerant (water needs to be removed); •Long reaction time (300 min)</p>

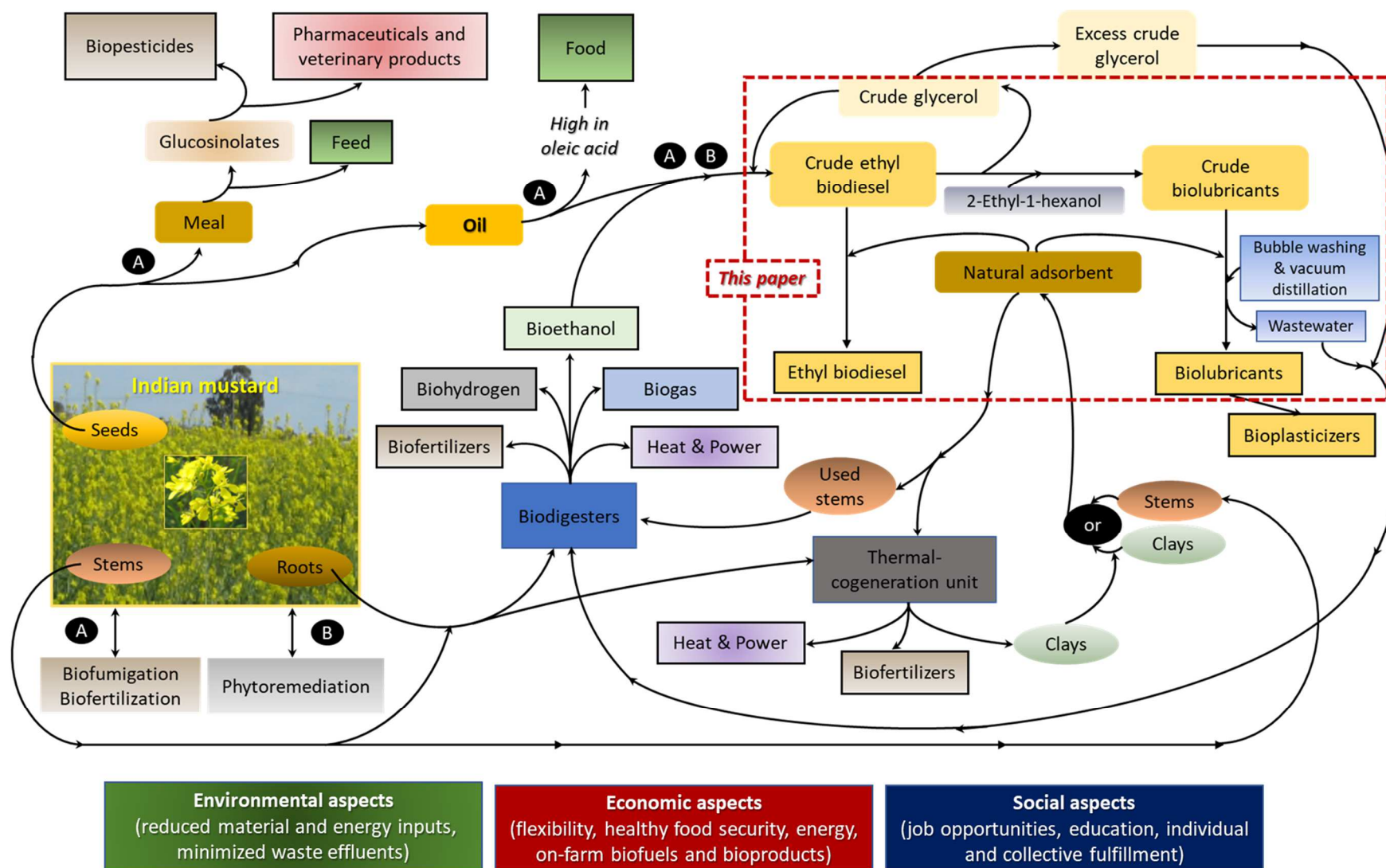
Table 8. Continued.

Feedstock	Conversion method	Advantages	Drawbacks
Triglycerides (from non-edible oils, waste cooking oil)	1.3-Lipases	<ul style="list-style-type: none"> •Easily separated; •Efficient; •Mild reaction conditions (40°C, 0.1 MPa); •Moderate energy consumption 	<ul style="list-style-type: none"> •Easily inactivated by methanol and deactivated by glycerol (both need to be removed); •High catalyst cost; •Long reaction time (1500 min)
	1.4-Non-catalytic supercritical method	<ul style="list-style-type: none"> •No chemical waste production; •Products with high purity; •Feedstock flexibility (water content > 50 wt%; reaction autocatalyzed by FFAs) 	<ul style="list-style-type: none"> •High reaction conditions (400°C, 20 MPa); •High capital investment and manufacturing costs
	2- Catalytic hydroprocessing (hydrodeoxygenation, decarbonylation, decarboxylation) to produce long-chain hydrocarbons, known as “renewable diesel”	<ul style="list-style-type: none"> •Drop-in fuel with high cetane number improving combustion performance (with a shorter ignition delay reducing the pre-mixed combustion stage) and emissions (with lower NOx formation) compared to petrodiesel 	<ul style="list-style-type: none"> •High temperature (250°C - 450°C); High pressure (4.5 MPa - 15 MPa); •High hydrogen to oil ratio (700 Nm³/m³)

Table 9. Main characteristics of methods used to produce biolubricants, i.e. lubricants derived from plant oils or animal fats (Syahir et al., 2017; Chen et al., 2019).

Conversion method	Advantages	Drawbacks
<i>Transesterification:</i> 1-Alcoholysis of TGs with a short alcohol to obtain fatty acid alkyl esters as well as glycerol; commonly, alkyl = methyl, leading to the commercialized (methyl) biodiesel ^a ; 2-Alcoholysis of the resulting biodiesel with a long-chain alcohol	<ul style="list-style-type: none"> •Two steps procedure; •Flexibility for biodiesel manufacturers to adapt their production and vary their sales markets; •Use of a wide variety of long-chain alcohols for leading to biolubricants with varying properties (2EH recommended); •Possibility of decreasing the reaction temperature by operating under high vacuum achieved using an ejector on an industrial scale 	<ul style="list-style-type: none"> •High oleic acid feedstock (to produce biolubricants meeting the desired properties); •Relatively high reaction temperature (110°C - 180°C) under reduced pressure (30 Pa - 5000 Pa)
<i>Estolide formation route:</i> 1-Alkaline hydrolysis of TGs to obtain FFAs as well as glycerol; 2-Bonding between the carboxylic acid functionality of a FFA and the double bond C=C of another FFA	<ul style="list-style-type: none"> •Two steps procedure; •Lower reaction temperature than for transesterification (50°C – 130°C); 	<ul style="list-style-type: none"> •Requires expensive capping fatty acids; •Strong acid catalyst; •Corrosive
<i>Epoxidation, ring opening and acetylation:</i> 1-Reaction of the TG double bond C=C with hydrogen peroxide in the presence of formic or acetic acid to form epoxide functional group (three-atom cyclic ether); 2-Catalytic reaction of the epoxidized TG with an alcohol to open the cyclic ether ring and form a hydroxyl group and an alkoxy group; 3-Esterification of the hydroxyl group formed in step 2- with acetic hydride to obtain the desired acetylated TG with release of acetic acid	<ul style="list-style-type: none"> •Lower reaction temperature than for transesterification (30°C – 150°C); •Final product exhibiting ideal lubricant properties 	<ul style="list-style-type: none"> •Multiple reaction stages (at least 3); •Corrosive; •High production costs

^a See **Table 8** for further details.



Graphical abstract